Neurobiology of Disease 124 (2019) 276–288

Contents lists available at ScienceDirect

Neurobiology of Disease

journal homepage: www.elsevier.com/locate/ynbdi

Development of an aggregate-selective, human-derived α-synuclein antibody BIIB054 that ameliorates disease phenotypes in Parkinson's disease models

Andreas Weihofen[a,b,*], YuTing Liu[a], Joseph W. Arndt[a], Christian Huy[b], Chao Quan[a], Benjamin A. Smith[a], Jean-Luc Baeriswyl[b], Nicole Cavegn[b], Luzia Senn[b], Lihe Su[a], Galina Marsh[a], Pavan K. Auluck[a], Fabio Montrasio[b], Roger M. Nitsch[b,c], Warren D. Hirst[a], Jesse M. Cedarbaum[a], R. Blake Pepinsky[a], Jan Grimm[b], Paul H. Weinreb[a,*]

[a] Biogen, 225 Binney Street, Cambridge, MA 02142, USA
[b] Neurimmune AG, Wagistrasse 13, 8952 Schlieren, Switzerland
[c] Institute for Regenerative Medicine, University of Zurich, Wagistrasse 12, 8952 Schlieren, Switzerland

ARTICLE INFO

Keywords:
Alpha-synuclein
Parkinson's disease
Lewy Bodies
Immunotherapy
BIIB054

ABSTRACT

Aggregation of α-synuclein (α-syn) is neuropathologically and genetically linked to Parkinson's disease (PD). Since stereotypic cell-to-cell spreading of α-syn pathology is believed to contribute to disease progression, immunotherapy with antibodies directed against α-syn is considered a promising therapeutic approach for slowing disease progression. Here we report the identification, binding characteristics, and efficacy in PD mouse models of the human-derived α-syn antibody BIIB054, which is currently under investigation in a Phase 2 clinical trial for PD. BIIB054 was generated by screening human memory B-cell libraries from healthy elderly individuals. Epitope mapping studies conducted using peptide scanning, X-ray crystallography, and mutagenesis show that BIIB054 binds to α-syn residues 1–10. BIIB054 is highly selective for aggregated forms of α-syn with at least an 800-fold higher apparent affinity for fibrillar versus monomeric recombinant α-syn and a strong preference for human PD brain tissue. BIIB054 discriminates between monomers and oligomeric/fibrillar forms of α-syn based on high avidity for aggregates, driven by weak monovalent affinity and fast binding kinetics. In efficacy studies in three different mouse models with intracerebrally inoculated preformed α-syn fibrils, BIIB054 treatment attenuated the spreading of α-syn pathology, rescued motor impairments, and reduced the loss of dopamine transporter density in dopaminergic terminals in striatum. The preclinical data reported here provide a compelling rationale for clinical development of BIIB054 for the treatment and prevention of PD.

1. Introduction

Parkinson's disease (PD) is the second most common neurodegenerative disorder, affecting 1–2% of individuals over the age of 60. PD is characterized by progressive loss of dopaminergic neurons in the substantia nigra, as well as other types of neurons in the central, peripheral and enteric nervous systems. A pathological hallmark of PD is the presence of neuronal inclusions known as Lewy Bodies and Lewy Neurites that are enriched in aggregated forms of α-synuclein (α-syn) (Goedert et al., 2013; Spillantini et al., 1997). The propensity of α-syn to misfold and aggregate seems to be related to the loss of dopaminergic and other neurons in PD. Genetic studies link missense mutations in the gene encoding α-syn (*SNCA*) and elevated *SNCA* gene dosage to autosomal dominant forms of PD (Chartier-Harlin et al., 2004; Ibanez et al., 2004; Kruger et al., 1998; Polymeropoulos et al., 1997; Singleton et al., 2003). Genome-wide association studies have identified *SNCA* as one of

Abbreviations: α-syn, Alpha-synuclein; BAC, bacterial artificial chromosome; BSA, bovine serum albumin; CSF, cerebrospinal fluid; DAT, dopamine transporter; DLB, dementia with Lewy bodies; ECL, enhanced chemiluminescence; EDTA, ethylenediaminetetraacetic acid; EC50, half maximal effective concentration; HRP, horseradish peroxidase; IgG, immunoglobulin G; ITC, isothermal titration calorimetry; mAb, monoclonal antibody; Ac-α-syn, N-terminal acetylated α-syn; PD, Parkinson's Disease; PFF, preformed fibril; RT, room temperature; SEC, size exclusion chromatography; SDS-PAGE, sodium dodecyl sulfate-polyacrylamide gel electrophoresis; SNCA, alpha-synuclein gene; tg, transgenic; wt, wild type

* Corresponding authors at: Biogen, 225 Binney Street, Cambridge, MA 02142, USA.
E-mail addresses: andreas.weihofen@biogen.com (A. Weihofen), paul.weinreb@biogen.com (P.H. Weinreb).

https://doi.org/10.1016/j.nbd.2018.10.016
Received 25 August 2018; Received in revised form 23 October 2018; Accepted 26 October 2018
Available online 28 October 2018

the strongest risk loci associated with sporadic PD and elevated α-syn expression has been demonstrated for some risk variants (Cronin et al., 2009; Nalls et al., 2014; Soldner et al., 2016). The distribution of Lewy pathology in the nervous system relates to the presence of key motor, psychiatric, and cognitive symptoms of PD (Braak et al., 2003). Braak et al. (2003) have postulated that the pathology spreads throughout the brain in a stereotypic manner with disease progression. There is now strong evidence that cell-to-cell propagation of aggregated α-syn is the underlying mechanism for Lewy pathology spreading and thus for PD progression (Brettschneider et al., 2015; Goedert, 2015; Lee et al., 2010). This propagation involves the release of aggregated α-syn by neurons into extracellular space and uptake by other neurons, from which the aggregated α-syn can act as a seed to induce further α-syn misfolding and subsequent cycles of α-syn aggregate formation and release.

Most currently approved therapies for PD target dopamine-related deficiencies and none are disease modifying. The connection of α-syn to disease pathology and progression makes it one of the most compelling targets for the development of disease modifying therapies for PD (Brundin et al., 2017; Dehay et al., 2015). Active and passive immunotherapies against α-syn have been shown to reduce α-syn pathology and associated deficits in rodent models (George and Brundin, 2015; Schneeberger et al., 2016; Valera and Masliah, 2013). A phase 2 study (NCT03100149) with PRX002 (RG7935), a humanized version of mouse monoclonal antibody (mAb) 9E4 (Masliah et al., 2011), started in 2017 after demonstrating favorable safety, tolerability and pharmacokinetics in early-phase clinical studies (Jankovic et al., 2018; Schenk et al., 2017). 9E4 treatment in a preclinical model prevented the formation of C-terminal truncated α-syn, in a mechanism postulated to involve blocking calpain cleavage in this region of the protein (Games et al., 2014). BIIB054, the topic of this report, is currently being evaluated in a Phase 2 clinical trial ("SPARK", NCT03318523) after favorable safety, tolerability and pharmacokinetic studies in healthy controls and PD patients (Brys et al., 2018; Brys et al., 2017). Additional antibody-based therapies are in advanced stages of preclinical development (Brundin et al., 2017), and two vaccines comprising short peptides mimicking a region of α-syn, termed AFFITOPES® PD01A and PD03A, have been investigated in Phase 1 clinical trials for their tolerability and safety (Schneeberger et al., 2016).

Here, we describe the identification and characterization of a human-derived α-syn antibody (BIIB054) that has unique properties compared to previously reported antibodies. BIIB054 binds to a N-terminal epitope on α-syn, is highly selective for aggregated forms of α-syn, and displays beneficial treatment effects in α-syn preformed fibril (PFF) inoculation mouse models. In particular, the high selectivity of BIIB054 for oligomeric and fibrillar aggregates of α-syn may provide an optimal therapeutic benefit-risk profile by preferentially targeting the pathologically relevant toxic forms of α-syn.

2. Materials and methods

2.1. Antibodies

Antibodies used in this study were mouse monoclonal syn-1 to α-syn (clone 42, Becton-Dickinson), mouse monoclonal LB509 to α-syn (Abcam ab27766), rabbit monoclonal EP1536Y to pSer129 α-syn (Abcam Ab51253), a rabbit polyclonal to pan-synuclein (Abcam ab6176), rat monoclonal clone DAT-Nt to dopamine-transporter (EMD Millipore), murine monoclonal 9E4 to α-syn (generated from publicly available sequence information) and murine monoclonal P1.17 (isotype control IgG2a, produced using ATCC cell line TIB-10). Generation of BIIB054 and other human-derived antibodies are described below.

2.2. Generation of human-derived α-syn antibodies

BIIB054 and other human-derived α-syn antibodies (Table 1) were derived from de-identified blood lymphocytes collected from healthy elderly individuals with no signs of neurodegenerative disorders, using a similar clone selection strategy as previously described (Sevigny et al., 2016). Memory B-cells, isolated from peripheral blood lymphocyte preparations by anti-CD22-mediated sorting were cultured on gamma-irradiated human peripheral blood mononuclear cell feeder layers. Supernatants from isolated B-cells were screened for their ability to bind α-syn in a direct ELISA format using recombinant α-syn (2 μg/ml) coated to 96-well plates. B-cell conditioned medium was preabsorbed for 1 h at room temperature (RT) with 10% heat-resistant *E. coli* proteins in 1% bovine serum albumin (BSA). The preabsorption step was used to eliminate false positive hits such as those arising from sticky antibodies. Selected α-syn-reactive B-cell clones were subjected to cDNA cloning of IgG heavy and κ or λ light chain variable region sequences, and sub-cloned in expression constructs using Ig-framework specific primers for human variable heavy and light chain families in combination with human J-H segment-specific primers. BIIB054 was engineered to incorporate glycosylated human IgG1 heavy and human lambda light chain constant domain sequences. A murine chimeric IgG2a/lambda version of BIIB054 (chBIIB054) was generated for use in chronic efficacy studies in mouse models. Detailed methods for antibody purification and fragment crystallizable region (Fab) generation are outlined in supplementary data.

2.3. Animals

Wild type (WT) mice (C57BL/6JRccHsd) were obtained from Harlan Laboratories (Netherlands, now known as Envigo). Transgenic (tg) α-syn A53T (M83) mice expressing human α-syn A53T under the Prp promoter (Giasson et al., 2002) and tg BAC α-syn A53T mice expressing human α-syn A53T under the endogenous promoter lacking the murine *SNCA* gene (Kuo et al., 2010) were obtained from Jackson Laboratory (Germany). All animal studies were approved by the Swiss Veterinary Office and were performed according to all state and federal regulations. For tissue collection, mice were perfused through the left ventricle with cold saline (0.9% NaCl) for approximately 2–3 min after anesthesia with ketamine/xylazine.

2.4. Human brain samples

Post mortem brain tissues of non-demented control donors and donors with clinical diagnosis of PD or Dementia with Lewy Bodies (DLB) were obtained from the Netherlands Brain Bank (NBB, Netherlands Institute for Neuroscience, Amsterdam, open access: www.brainbank.nl). Written informed consent for the use of the samples for research purposes and clinical information of donors was obtained by the NBB. Samples were received either as frozen or formalin-fixed paraffin embedded tissue. Age at death, gender, diagnosis, tissue source, and methods of analysis used in this study are summarized in Table S1.

2.5. Peptide arrays for epitope mapping

33 overlapping peptides spanning the entire sequence of human α-syn were synthesized (peptides were 15 residues in length with an overlap of 11 residues), and coupled via a flexible linker to a cellulose membrane (PepSpots®, JPT, Germany). The membrane was rinsed in methanol, blocked with Rotiblock (Roth, Germany) for 1 h, and incubated with BIIB054 or 21D11 diluted in blocking solution for 1 h followed by horseradish peroxidase (HRP)-labeled secondary antibody for 1 h. Incubations were at RT and the membrane was washed 3× with phosphate-buffered saline (PBS) containing 0.1% Tween 20 (PBS-T) for 5 min between incubations. Blots were developed using enhanced chemiluminescence (ECL) from GE Healthcare.

2.6. Direct ELISA

To measure the EC_{50} for BIIB054 and BIIB054 Fab binding to α-syn, 100 µl of recombinant human α-syn protein at 1 µg/ml was coated overnight at 4 °C onto 96-well plates (NUNC MaxiSorp, Thermo Scientific) in PBS. The plates were decanted and blocked with 350 µl of PBS-T containing 1% BSA (Sigma) for 1 h at RT. BIIB054 or BIIB054 Fab was serially diluted to the indicated concentrations (100 µl/well) in duplicate. The plates were incubated for 1 h at RT. Binding was determined using an HRP-conjugated secondary antibody (Jackson ImmunoResearch) followed by measurement of HRP activity using 3,3′,5,5′-tetramethylbiphenyl-4,4′-diamine (Sigma). The reaction was stopped with 1 N H_2SO_4 and colorimetric analysis was performed using a Beckman Spectrophotometer at 450 nm. The plates were washed with 350 µl PBS-T four times by a plate washer between steps. A similar method was used for EC_{50} measurements of peptides except that the biotinylated peptides were captured onto streptavidin-coated clear 96-well plates (Pierce). For specificity and epitope analysis α-syn, β-syn, γ-syn and truncated forms of α-syn were purchased from rPeptide (Watkinsville, GA) and processed as described above except samples were coated onto 96-well half area microplates (Corning) in 0.1 M carbonate/bicarbonate pH 9.6 buffer and plates were blocked with PBS-T containing 2% BSA.

2.7. Isothermal titration calorimetry

BIIB054 antibody and Fab, and N-terminal acetylated α-syn (Ac-α-syn) were buffer exchanged into PBS using Zeba spin desalting columns (Thermo Fisher, 89890). The recombinant human Ac-α-syn was centrifuged at 600,000 *g* at 4 °C with a Beckman Coulter tabletop ultracentrifuge to remove potential aggregates. All protein concentrations were then calculated from absorbance measurements at 280 nm using extinction coefficients calculated from their primary amino acid sequences. The isothermal titration calorimetry (ITC) experiments were performed on a Microcal ITC200 calorimeter with a total of 20 injections of 2 µl each with 4 s duration, 150 s spacing. Data were analyzed using the Origin software package with a 1:1 fitting model.

2.8. X-ray crystallography

The BIIB054 Fab/α-syn peptide complex was prepared by mixing BIIB054 Fab (11 mg/ml) with a 5-fold molar excess of $\alpha\text{-syn}_{Ac1–10}$ (Ac-MDVFMKGLSK) peptide (ABclonal, Woburn, MA) in 20 mM sodium acetate pH 4.5, 200 mM NaCl. Crystallization was performed by the nanodroplet vapor diffusion method at 24 °C by mixing 200 nl of the complex with 200 nl of the reservoir solution containing 18% *w/v* PEG 3350, 17% w/v PEG 400, 4.8% *v*/v 2-propanol, and 100 mM 3-(cyclohexylamino)-2-hydroxyl-1-propoanesulfonic acid at pH 8.9. Crystals grew to full size (100 µm × 75 µm × 50 µm) in two weeks. The crystals were harvested under the oil-based cryoprotectant (66.5% (*w*/w) Paratone-N, 28.5% paraffin oil and 5% glycerol) (Sugahara and Kunishima, 2006) and flash-frozen in liquid nitrogen. Diffraction data were collected at beamline 31-ID of Advanced Photon Source at −173 °C using a MAR225 CCD detector, and processed in the monoclinic space group $P2_1$ using the program XDS (Kabsch, 2010). Data statistics are summarized in Table S2. The structure of the BIIB054 Fab/$\alpha\text{-syn}_{Ac1–10}$ complex was determined to 1.90 Å resolution by molecular replacement using the program MolRep (Vagin and Teplyakov, 1997) and the apo BIIB054 Fab structure as the search model (not shown). Well-defined electron density was observed for the entire $\alpha\text{-syn}_{Ac1–10}$ peptide, which was manually built with Coot (Emsley et al., 2010). Structure refinement was performed using Phenix (Adams et al., 2010). The final model includes 2 Fab molecules, two $\alpha\text{-syn}_{Ac1–10}$ peptides, and 538 water molecules in the asymmetric unit. The progress of the model refinement was monitored by cross-validation R_{free}, which was computed from a randomly assigned test set comprising 5% of the data. The final R factor is 18.0% with an R_{free} factor of 22.3%. Analysis of the stereochemical quality of the models was accomplished using the AutoDepInputTool (http://deposit.pdb.org/adit/). Crystal structures were also solved with BIIB054 Fab with non-acetylated $\alpha\text{-syn}_{1–10}$ peptide (MDVFMKGLSK) and non-acetylated $\alpha\text{-syn}_{1–10}$ peptide oxidized at M5 ($MDVFM_{Ox}KGLSK$) (data not shown), following the same procedure as described above. Figures were prepared with PyMOL (Schrodinger LLC). Atomic coordinates and experimental structure factors of the BIIB054 Fab/$\alpha\text{-syn}_{Ac1–10}$ complex have been deposited in the Protein Data Bank with the accession number 6CT7.

2.9. Generation of α-syn fibrils

α-syn protein was generated as described in detail in Supplementary data. For α-syn PFF generation, murine α-syn (at 10 mg/ml) and human α-syn (at 5 mg/ml) monomeric solutions were adjusted to contain 150 mM NaCl, divided into 0.2 ml aliquots in 1.7 ml microcentrifuge tubes and continuously shaken at 1100 rpm in a ThermoMixer C (Eppendorf) at 37 °C for 5 days. The resulting α-syn PFF solutions were aliquoted, stored at −80 °C and used for α-syn PFF inoculation mouse models. The α-syn PFFs were water-bath sonicated prior to injection.

For dot blot and ELISA analysis using human α-syn PFFs, 500 µl of human α-syn (at 5 mg/ml) was first cleared of aggregates by ultracentrifugation at 600,000 *g* for 30 min at 4 °C. The supernatant was transferred to a 1.7 ml Eppendorf tube and α-syn PFFs were formed by continuous shaking at 1000 rpm in an Eppendorf Thermomixer at 37 °C for 7 days. After the treatment, the remaining monomer was removed by pelleting the α-syn PFFs by centrifugation at 600,000 *g* for 40 min, resuspending the pellet to its original volume with PBS followed by three PBS/centrifugation wash steps. After each centrifugation, the supernatant was removed and the concentration of α-syn was calculated from absorbance measurements at 280 nm using a calculated extinction coefficient (ε280 0.1% = 0.35 per cm) based on the primary amino acid sequence. The concentration of α-syn PFFs was estimated by subtracting the total amount of α-syn in the supernatant from each of the three wash steps from the starting concentration prior to agitation.

2.10. Generation of multimeric α-syn by chemical cross-linking

Multimeric forms of α-syn were generated by a three-step cross-linking procedure as follows. First, thiol groups that could be used for cross-linking were incorporated into carboxyl groups on α-syn by incubating 100 µM α-syn with 40 mM cystamine-2HCl (Fisher) for 1 h at RT in 100 mM 2-(N-morpholino) ethanesulfonic acid (MES), pH 6.0, 0.5 M NaCl in the presence of 2 mM of 1-ethyl-3-[3-dimethylaminopropyl] carbodiimide (Thermo) and 5 mM sulfo-N-hydroxysuccinimide (Thermo). The resulting α-syn-cystamine conjugate was recovered from the reaction mixture on a Zeba spin desalting column. Next, reactive thiol groups were generated by reducing the disulfide bonds present in the conjugated cystamine with 0.1 mM dithiothreitol for 20 min at 37 °C. The excess chemicals were removed on a Zeba spin desalting column equilibrated in 10 mM MES, pH 5.0, 0.1 M NaCl. Finally, multimeric α-syn was formed by reacting 100 µM of the α-syn-cystamine conjugate with 25 µM tetravalent maleimide cross-linker (4-Arm PEG-MAL, Creative PEGWorks) with 25 mM MES, pH 6.5 added for 2 h at RT. After cross-linking, α-syn monomers, dimers, trimers, tetramers and pentamers were fractionated by SEC on a Superdex 200 column and relevant fractions identified by SDS-PAGE. Peak fractions were pooled and stored at −80 °C.

BIIB054 binding to the α-syn multimers was evaluated using a competition-based ELISA. 96-well plates (Nunc MaxiSorp) were coated with 100 µl/well of BIIB054 at 2 µg/ml in PBS at 4 °C overnight. The plates were decanted and blocked with 350 µl of PBS-T containing 1% BSA for 1 h at RT. α-Syn multimers were serially diluted to the indicated concentrations, added to the coated plates (100 µl/well) in duplicate, and incubated for 1 h at RT with gentle shaking. The plates

were decanted, without washing, and incubated with 100 µl/well of 5 µg/ml biotinylated α-syn PFF for 10 min and then with a 1:5000 dilution of streptavidin-HRP for 1 h at RT. HRP activity was measured as previously described in section 2.6. The plates were washed with 350 µl PBS-T four times by a plate washer between steps except where indicated.

2.11. Stereotaxic injections of α-syn PFFs and systemic treatment with chBIIB054 in mice

Unilateral stereotaxic intrastriatal injections of α-syn PFFs were performed as previously described (Luk et al., 2012a; Luk et al., 2012b). Human or mouse α-syn PFFs were used for studies in human α-syn tg mice or for non-tg mice, respectively, since previous studies have demonstrated that seeding occurs most efficiently when the α-syn PFFs and the target are the same species of α-syn (Luk et al., 2012a; Luk et al., 2012b). In short, 2–3 month old mice were anesthetized and stereotaxically injected with α-syn PFFs at a rate of 0.2 µl per min (2 µl total volume for WT and tg BAC α-syn A53T and 2.5 µl total volume for M83 mice) into the right forebrain to target inoculum to the dorsal neostriatum (+2.6 mm beneath the dura: 3.2 mm including skull; AP +0.2 mm, ML +2.0 mm, DV −2.6 mm). Animals received 30 mg/kg doses of chBIIB054 or control IgG, or vehicle via intraperitoneal (i.p.) injections 2–3 times prior to α-syn PFF injection and weekly post-injection until time of sacrifice. Detailed study outlines, including mouse strain, gender, treatment schedules, and α-syn PFF details are listed in Table S3.

2.12. Phenotype assessment in α-syn PFF-inoculated M83 mice

Onset of first symptoms of paralysis, severe paralysis and weight loss in α-syn PFF-inoculated heterozygous tg α-syn A53T (M83) mice were analyzed by Kaplan-Meier survival plot analysis. Examiners were blinded to treatment. Mice were weighed every second week and the date of maximum weight was recorded. Mice were evaluated three times a week according to a general predefined health assessment protocol. The first signs of paralysis were indicated by irregularity of gait, limping or dragging of hindlimbs. Events were recorded only if initial symptoms were confirmed at least once during the next three phenotype assessments. Mice were euthanized and the date recorded when an animal's health was severely affected by paralysis (lying on side, complete paralysis of hindlimbs). Animals were excluded if their health impairment was not due to paralysis. Mantel-Cox test was used for statistical analysis.

2.13. Wire hang test

Mice were placed on a cage lid, which was inverted, lightly shaken and suspended 50 cm above the home cage. The hang area on lid was 10 × 10 cm and the wires were 2 mm thick. The latency-to-fall time was recorded. The trial was stopped if a mouse remained on the lid for longer than 14 min. Each animal completed two trials with a 2 min recovery time between trials. Reported endpoint is the average of the two trials. The examiner was blinded to the treatment. Student's *t*-test was used for statistical analysis.

2.14. Tissue homogenization for Western blot analysis

Homogenizations were conducted using FastPrep®-24 device for 60 s at 6.5 m/s with Lysing Matrix D tubes (MP Biomedicals). All buffers were supplemented with Complete Mini protease inhibitor cocktail and PhosSTOP phosphatase inhibitor cocktail (Roche Diagnostics).

For striatal dopamine transporter (DAT) analysis in mice, ipsilateral and contralateral striata were collected using a mouse brain slicer (TED PELLA inc, coronal, 1 mm spacing, cut between spacer 4 and 5) and weighed. Dissected striata were homogenized in 36 volumes (*v/w*) RIPA buffer (50 mM Tris-HCl pH 7.4, 150 mM NaCl, 1 mM EDTA, 1% Nonidet P40, 0.5% sodium deoxycholate, 0.1% SDS). The lysates were cleared by centrifugation at 16,100 *g* for 30 min at 4 °C, and stored at −80 °C for analysis by Western blotting.

For α-syn analysis in mice, cortices of left hemisphere were dissected, homogenized, and sequentially treated with high salt, Triton X-100 and SDS wash/extraction steps. First, cortices were homogenized in 8 volumes (v/w) 50 mM HEPES-KOH pH 7.6, 750 mM NaCl, 5 mM EDTA (Buffer A). 600 µl Buffer A lysates were centrifuged at 16,100 *g* for 45 min at 4 °C. After washing, the pellets were resuspended in 600 µl 50 mM HEPES-KOH pH 7.6, 1% Triton X-100, 750 mM NaCl, 5 mM EDTA (Buffer B) and incubated on ice for 15 min before centrifugation 16,100 *g* for 45 min at 4 °C. This pellet was resuspended in 300 µl 50 mM HEPES-NaOH 7.6, 1% SDS (Buffer C) and incubated at RT for 30 min. Where indicated, the SDS (Buffer C) insoluble fraction was cleared by centrifugation (16,100 *g* for 30 min at RT) and the pellet was resuspended in 75 µl of 50 mM Tris-HCl pH 7.5 in 8 M urea. Total protein concentration was determined using a Pierce BCA Protein Assay Kit (Thermo). Samples were stored at −80 °C for Western blot analysis.

2.15. Western blot analysis of tissue homogenates

Brain tissue lysates normalized for total protein concentration were subjected to SDS-PAGE on Bis-Tris NuPAGE 4–12% gradient gels under reducing conditions and transferred to polyvinylidene difluoride membranes. Membranes for α-syn analysis were fixed with fresh 0.4% paraformaldehyde in PBS for 30 min. Membranes were incubated with primary antibodies (syn-1 for full-length and ~ 6 kDa α-syn variants, EP1536Y for pSer129 α-syn and clone DAT-Nt for DAT), then with HRP-conjugated secondary antibodies, and finally with ECL plus substrate (GE Healthcare). HRP activity was imaged using a chemiluminescence imager (Bio-Rad). Each sample was analyzed at least 2 times on independent blots. Image J was used for quantification of full-length, pSer129 α-syn and α-syn 6 kDa and Image Lab Software (BioRad) was used for DAT. Membranes were washed 3× with PBS-T for 5 min between incubations. The reported endpoints are the normalized ratios of α-syn 6 kDa or pSer129 α-syn (~ 14 kDa band) to full length α-syn. Control group values were set to 100% and statistical analysis was done using a mixed model setting treatment effect as fixed variance and day-to-day variance of α-syn PFF inoculation as random effect. For DAT analysis, the reported endpoint is percentage ipsilateral relative to contralateral DAT levels and Mann-Whitney test was applied for statistical analysis.

2.16. Dot blot assay with human tissue homogenate

Frozen human post mortem brain tissues (~ 200 mg) were homogenized in 8 volumes (*v/w*) 50 mM HEPES KOH pH 7.6, 750 mM NaCl, 5 mM EDTA, protease and phosphatase inhibitors (Halt, Pierce) with Lysing Matrix D beads using FastPrep®-24 homogenizer (MP Biomedical) for 60 s at 6.5 m/s. Total protein concentrations were determined by BCA assay (Pierce). Brain homogenates were spotted onto 0.45 µm nitrocellulose membranes (2 µl of 100 ng/µl and 1 µg/µl total protein of amygdala and substantia nigra homogenates, respectively). The membranes were air dried for 30 min, blocked in 5% non-fat milk TBS-T, and probed with primary antibodies chBIIB054 or 9E4 (1.25 µg/ml), followed by HRP-conjugated goat-anti mouse IgG. Blots were washed 3× with TBS-T for 10 min between incubation steps, developed using ECL substrate and imaged using a ChemiDoc imaging system (BioRad).

2.17. Dot blot assay with recombinant protein

A Bio-Dot apparatus (Bio-Rad) was assembled with a pre-wet 0.2 µm nitrocellulose membrane following the manufacturer's protocol. 100 µl of a 2-fold dilution series of α-syn PFFs or monomer was applied,

incubated for 5 min and then vacuum was applied. The wells were washed with 200 µl TBS-T twice under vacuum and the membrane was air dried completely. The dried membrane was blocked with 2% non-fat dry milk TBS-T for 1 h at RT. The membrane was cut into the experimental segments and incubated with 1 µg/ml primary antibody in PBS-T for 1 h and then with a 1:5000 dilution of IRDye® 680RD Donkey anti-mouse (LI-COR) or IRDye® 800CW Goat anti-human (LI-COR) secondary antibody for 1 h at RT. Three washes with PBS-T were performed after each incubation. The blot was imaged using an Odyssey® CLx Infrared Imaging System (LI-COR).

2.18. Immunohistochemistry

Immunohistochemistry was performed on formalin-fixed, paraffin-embedded samples of amygdala/temporal cortex and substantia nigra from post mortem human brains from non-demented control donors and donors with PD or DLB. Five-micron sections were prepared. Single sections were immunostained with antibody EP1536Y (3.5 µg/ml), LB509 (0.5 µg/ml), 9E4 (2 µg/ml) and chBIIB054 (2 or 8 µg/ml) using Ventana Discovery Ultra immunostainers (Ventana Medical Systems, Inc., Tucson, AZ). Ventana CC1 (EDTA buffer) was used for epitope retrieval, Ventana OmniMap anti-mouse and OmniMap anti-rabbit HRP-conjugated reagents were used as secondary antibodies. Ventana Purple chromogen was used to detect the immunoreactivity; sections were counterstained with hematoxylin. Immunostained slides were digitized on a 3D-Histech Pannoramic-250 whole slide scanner (Perkin Elmer), at 20× magnification.

2.19. Pharmacokinetics

Pharmacokinetics of BIIB054 were performed in male C57BL-6 mice (n = 4/group). Blood samples were obtained at 1 h, 3 h, 8 h, 24 h, 3 d, 5 d, 10 d, 14 d, 21 d and 28 d following a single 10 mg/kg intraperitoneal (i.p.) injection and at 15 min, 1 h, 8 h, 24 h, 4 d, 7 d, 10 d, 14 d, 21 d and 28 d following a single intravenous (i.v.) injection. Plasma titers were determined by ELISA using a donkey anti-human Fcγ specific capture antibody. Pharmacokinetic parameters were calculated by non-compartmental analysis using WinNonlin Software (WinNonlin, Pharsight Inc., Mountain View, CA).

3. Results

3.1. Generation of human-derived α-syn binding antibody BIIB054

Autoantibodies against α-syn are found in healthy elderly individuals (Besong-Agbo et al., 2013; Horvath et al., 2017). Based on the hypothesis that some endogenous antibodies could be protective, we identified a panel of α-syn binding antibodies by screening memory human B-cell libraries from healthy elderly individuals with no signs of neurodegenerative disorders (Jelcic et al., 2015; Sevigny et al., 2016). Culture supernatants were screened for the presence of antibodies that bind α-syn by ELISA. IgG heavy and light chain variable region sequences were cloned from α-*syn*-reactive B-cell clones, and functional antibodies engineered from these sequences were produced in CHO cells. Antibodies binding different epitopes within α-syn and displaying various specificities for α-syn were identified (Examples in Table 1 and Fig. S1), confirming that a wide range of α-syn-reactive antibodies are present in the immune repertoires of this population. BIIB054 was selected for additional studies based on its lack of cross-reactivity with β- and γ-syn, strong binding to immobilized α-syn by ELISA, and high selectivity for aggregated forms of α-syn (discussed below).

Table 1
Properties of α-syn antibodies derived from human B-cell screening.

Antibody	Specificity			Epitope
	α-syn	β-syn	γ-syn	
12F4 (BIIB054)	yes	no	no	N-terminal (1 – 10)
21D11	yes	no	no	C-terminal (117–123)
11E1	yes	yes	no	Mid-region (61–95)
34E10	yes	yes	yes	N-terminal (1–60)
3G12	yes	no	no	Conformational

3.2. BIIB054 binds to the N terminus of α-syn

The specificity of BIIB054 for α-syn was assessed using an ELISA format on plates coated with α-, β-, or γ-synuclein. BIIB054 selectively bound α-syn but not β- or γ-synuclein, whereas a control pan-synuclein antibody bound all three synuclein family members (Fig. 1A). The epitope for BIIB054 was identified by immunoblotting on a peptide array (Fig. 1B). From an analysis of 33 overlapping linear 15-mer peptides covering the entire α-syn sequence, BIIB054 only bound to peptide A1, localizing its reactivity to within the N-terminal 15 amino acids of α-syn. This sequence of human α-syn is fully conserved across several species, including mouse, cynomolgus monkey, rat, and rabbit, and cross-reactivity with each of these α-syn sequences was confirmed experimentally using recombinant proteins (not shown).

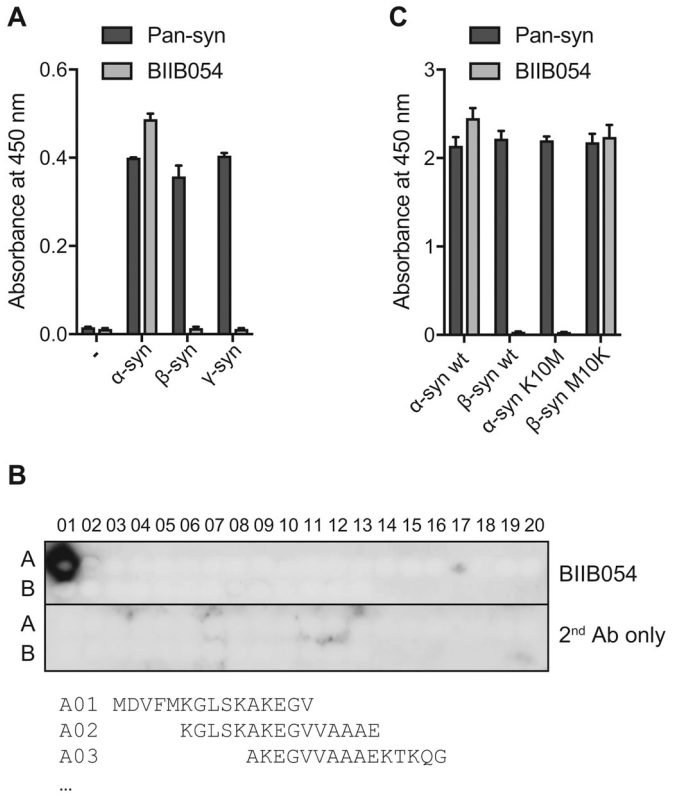

Fig. 1. BIIB054 binds specifically to the N terminus of α-syn. (A) Direct ELISA showing the binding of BIIB054 and rabbit polyclonal pan-synuclein positive control antibody to 96-well plates coated with 2 µg/ml α-, β- or γ-syn (mean values with error bars, n = 2). (B) Immunoblot analysis of 33 overlapping linear 15-mer peptides covering the entire α-syn protein (positions A01 to A20 and B01 to B13) probed with and without BIIB054. (C) Direct ELISA showing BIIB054 binding to plates coated with recombinant α-syn, β-syn, α-syn K10 M and β-syn M10 K fragments (residues 1–60) (mean values with error bars, n = 2).

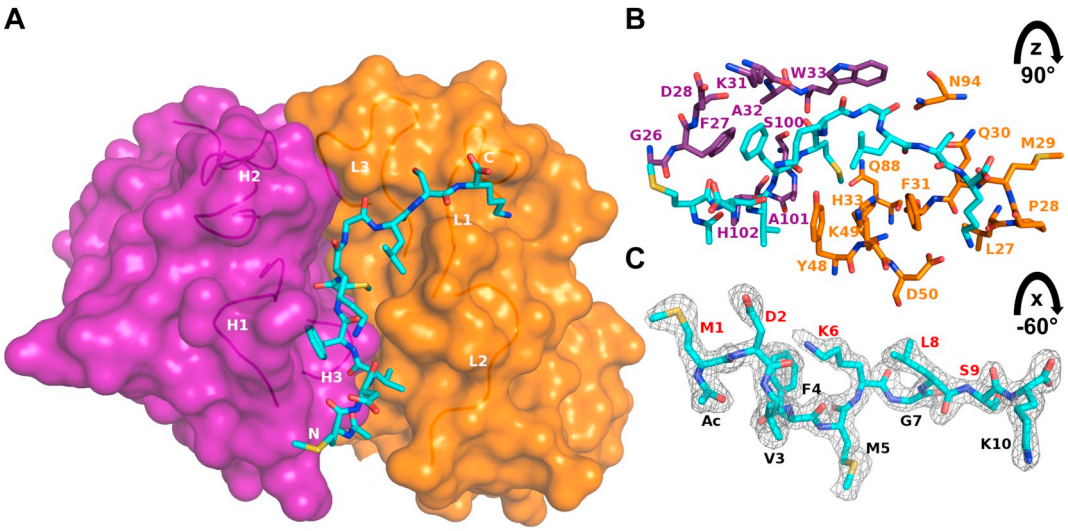

Fig. 2. Crystal structure of BIIB54 Fab with acetylated- α-syn peptide 1–10. (A) Top view of the BIIB054 Fab in surface representation looking down onto the binding paratope (HC, purple; LC, orange), Ac-α-syn peptide in cyan. (B) Detailed view of the binding interface with key interface residues of BIIB054 within 4 Å of the Ac-α-syn peptide shown and labeled. (C) α-syn peptide conformation seen bound to BIIB054 Fab in the structure superposed with an omit electron density map contoured at 3.0 σ, shown as mesh. Critical and non-critical residues identified by alanine scanning are shown in black and red text, respectively.

Most antibodies that bind near the N terminus of α-syn cross-react with β-synuclein (β-syn) (Dhillon et al., 2017; Waxman et al., 2008) due to the high degree of sequence identity between α-syn and β-syn in this region. Lysine (K10), which forms part of the binding site of BIIB054, is replaced by methionine (M10) in β-syn and is the only sequence difference between α-syn and β-syn within residues 1–26. To test if this residue alone accounts for the selectivity of BIIB054 for α-syn, we generated a K10 M-containing version of α-syn and a M10 K-containing version of β-syn and tested them for BIIB054 binding in a direct ELISA. The K10 M mutation in α-syn completely abolished BIIB054 binding, whereas the reverse M10 K mutation in β-syn led to BIIB054 binding (Fig. 1C), confirming this lysine as the key determinant for the observed specificity for α-syn.

3.3. Structure of BIIB054 in complex with α-syn

To explore the molecular basis for antigen recognition, we determined the crystal structure of the BIIB054 Fab in complex with Ac-α-syn peptide 1–10 at 1.9 Å resolution (Fig. 2A). The crystallographic data are summarized in Table S1. Residues 1–10 of Ac-α-syn adopt a well-defined, L-shaped conformation that span ~25 Å with residues 1–6 being roughly perpendicular to residues 7–10. The Ac-α-syn peptide has a total surface area of 1510 Å^2, of which ~55% (823 Å^2) is buried at the interface with the BIIB054 Fab with high shape complementarity (0.79). The α-syn binding site of BIIB054 is primarily formed of CDRs H1, H3 of the heavy chain and L1, L2, L3 of the light chain (Fig. 2A and B). Some notable structural features of this interface include the complementary hydrophobic and π-stacking contacts made by the side chains V3, F4, M5 and G7 of Ac-α-syn that bury into the VH/VL interface of BIIB054 (Fig. 2A and B). Additionally, the charged side chain K10 of Ac-α-syn is close to the oppositely charged residue D50 of the BIIB054 light chain forming an electrostatic interaction and at least 6 hydrogen-bonds are found between main-chain atoms of α-syn with residues W33, S100, H102 (heavy chain) and M29, Y48, N94 (light chain) of BIIB054. Collectively these interactions contribute to stabilizing of the complex. The α-syn peptide shows clear electron density in an unbiased composite omit map (Fig. 2C). Critical residues of the BIIB054 epitope are located on the same side of the peptide forming a contiguous binding surface. In contrast, the side chains of M1, D2, K6, L8, and S9 are on the opposite side of the peptide extending away from BIIB054 toward the solvent and do not interact with the antibody (Fig. 2C). The importance of the molecular contacts seen between BIIB054 and Ac-α-syn 1–10 was substantiated by alanine scanning mutagenesis in an ELISA format, using α-syn peptides containing single alanine substitutions for residues M1 – K10 (Fig. S2A). Alanine substitution of V3, F4, M5, or G7 reduced BIIB054 binding, while mutation of K10 eliminated binding. Substitutions of M1, D2, L8, or S9 with alanine did not impact binding, confirming that these side chains are not part of the binding epitope.

An unexpected feature of the structure is that the binding interface is highly hydrated with at least 15 interfacial waters, which form a complex hydrogen bonding network bridging α-syn with BIIB054 (Fig. S3A). Interestingly, five of the water molecules cluster around the M5 side chain forming a spacious pocket at the VH/VL interface of sufficient size to accommodate oxidation of the methionine (Fig. S3B). From an analysis of the binding of BIIB054 to α-syn with and without oxidized M1 and M5, we confirmed binding and in fact observed a slight preference for binding of BIIB054 to oxidized α-syn (Fig. S2B).

The structure also reveals a H-bond between the H102 side chain of the BIIB054 heavy chain and the acetyl group carbonyl oxygen on M1 of the Ac-α-syn peptide (Fig. S3C). A second crystal structure was solved with BIIB054 Fab with non-acetylated α-syn 1–10. Its overall structure was nearly identical to the Ac-α-syn bound structure ($RMSD_{overall}$ 0.1 Å), except for a large conformational rearrangement of Met 1 of α-syn, due to the rotation of the psi dihedral angle, and an 0.5 Å shift in the side chain of H102 of BIIB054 (Fig. S3D). From ELISA studies of full-length α-syn expressed with and without the M1 acetyl group, we observed an 8-fold higher affinity of BIIB054 for the acetylated protein (Fig. S2B), confirming the importance of the contacts between M1 and BIIB054 Fab observed in the structure of the acetylated peptide. Taken together, the epitope mapping results establish that BIIB054 binds residues M1 to K10 of the α-syn peptide, and suggest a preference for acetylated and oxidized forms of α-syn.

3.4. BIIB054 selectively binds aggregated forms of recombinant α-syn

Previous studies have shown that some N-terminal α-syn antibodies preferentially bind pathological aggregated forms of α-syn (Dhillon et al., 2017; Duda et al., 2002; Waxman et al., 2008). The mechanistic basis for this preferential binding is unknown. The affinity of BIIB054 for monomeric Ac-α-syn was determined in solution by ITC. A K_D value of ~ 100 nM was calculated from a titration of BIIB054 at a fixed Ac-α-

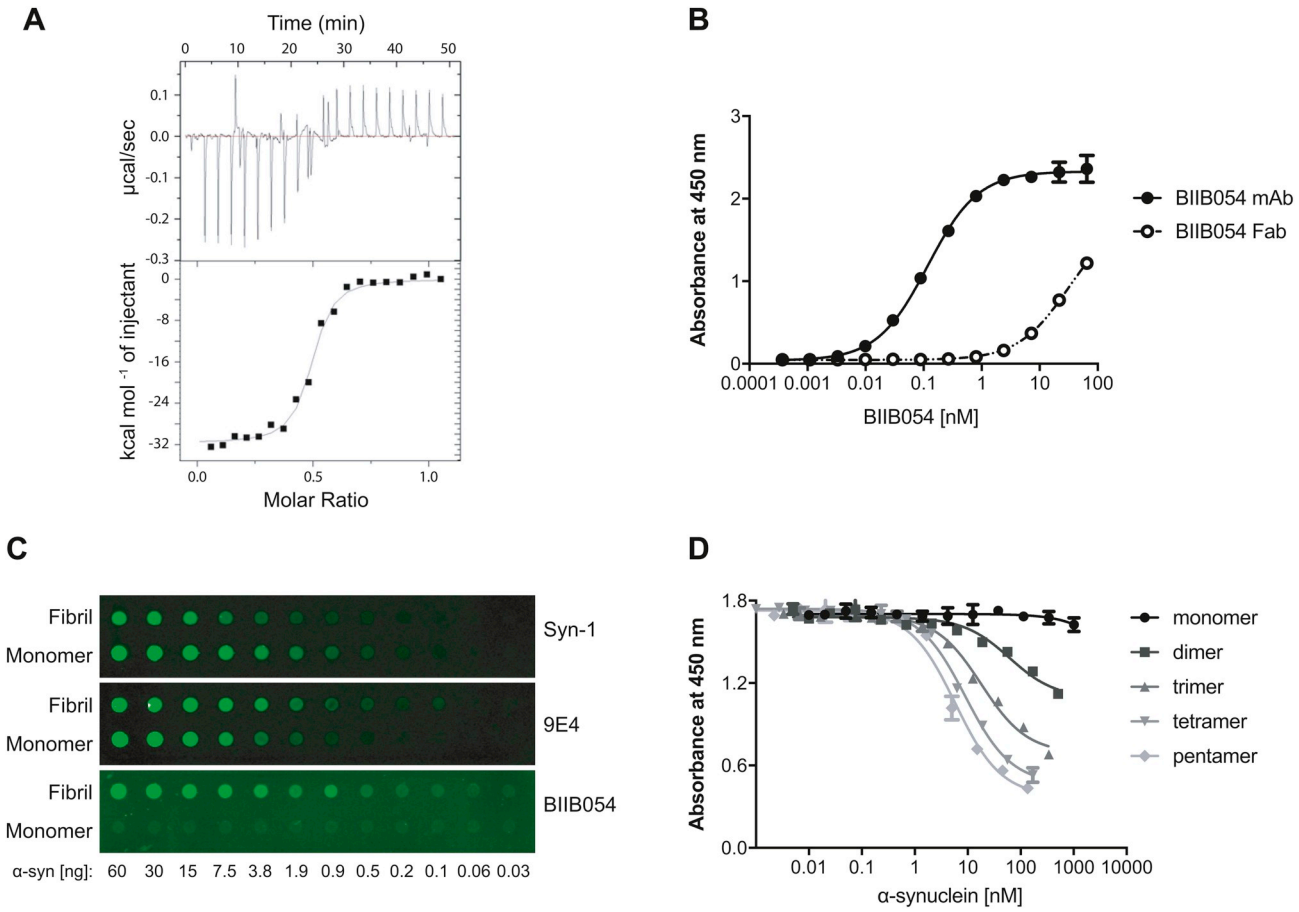

Fig. 3. BIIB054 selectively binds aggregated recombinant α-syn. (A) Isothermal titration calorimetry binding analysis of serial dilutions of BIIB054 to a fixed concentration of recombinant monomeric α-syn. Upper panel shows the heat flow. Lower panel shows the heat of injection as a function of molar antibody: α-syn ratio. (B) Direct ELISA showing binding of BIIB054 mAb and Fab to a 96-well plate coated with α-syn fibrils. Each point is the average of two measurement with error bars. (C) Dot blot analysis measuring the binding of BIIB054, 9E4 and syn-1 antibodies to recombinant α-syn fibrils and monomer. 2-fold serial dilutions of α-syn fibrils and monomer starting at 0.6 µg/ml were applied. (D) Competition ELISA showing concentration-dependent inhibition of the binding of BIIB054 to a 96-well plates coated with α-syn fibrils by α-syn monomers, dimers, trimers, tetramers, and pentamers.

syn concentration (Fig. 3A). An analysis of the binding of the monovalent BIIB054 Fab to Ac-α-syn by ITC similarly yield a K_D value of 100 nM (Fig. S4A and B). Analysis of BIIB054 Fab fragment binding to immobilized α-syn by surface plasmon resonance showed fast dissociation kinetics (k_{off} > 0.5/s) and a monovalent K_D of ~ 400 nM (Fig. S4C). To quantify the binding of the bivalent BIIB054 mAb to aggregated α-syn we used an ELISA. The EC_{50} from this analysis for BIIB054 mAb was ~120 pM (Fig. 3B), representing an approximately 800-fold higher apparent affinity for fibrillar α-syn than observed for monomeric Ac-α-syn using ITC. BIIB054 Fab was tested in the same assay (Fig. 3B). Binding of the monovalent BIIB054 Fab to fibrillar α-syn was too weak to be quantified with an accurate EC_{50}, but was > 100-fold lower than with the bivalent mAb. To further substantiate the binding preference of BIIB054, we performed a dot blot analysis in which serial dilutions of recombinant monomeric and fibrillar α-syn (0 to 60 ng) were applied to a nitrocellulose membrane and probed with BIIB054. BIIB054 showed a strong preference for α-syn fibrils (Fig. 3C bottom panel and Fig. S5). BIIB054 binding was detected with as little as 0.9 ng fibrillar α-syn spotted onto the membrane, but was only detected when ≥ 4 µg monomeric α-syn was applied. For comparison, we investigated the selectivity of the syn-1 (Perrin et al., 2003) and 9E4 (Masliah et al., 2011) antibodies. Syn-1 and 9E4 bound well to both monomeric and fibrillar α-syn in the dot blot format. Syn-1 showed a slight preference for monomeric α-syn (Fig. 3C top panel), whereas 9E4 showed a slight preference for fibrillar α-syn (Fig. 3C middle panel). The impact of valency on the binding of α-syn to BIIB054 was further assessed in a competition ELISA using α-syn monomer, dimer, trimer, tetramer, and pentamer that were generated by cross-linking (Fig. 3D and S6). In this assay format, monomeric α-syn showed only negligible inhibition even at the highest concentration tested. In contrast, dimeric α-syn conferred significant inhibition, which was further increased for higher order trimeric, tetrameric, and pentameric forms. Although the cross-linked α-syn multimers are not necessarily representative of the structure of pathological α-syn aggregates, the binding data provide clear evidence of the role valency plays in BIIB054 binding.

3.5. BIIB054 selectively binds pathological forms of α-syn in human brain

We next addressed if the selectivity of BIIB054 for recombinant aggregated α-syn over monomeric α-syn translated to preferential binding to pathological α-syn species in PD and DLB patients as compared to α-syn in brain tissues from individuals with no neuropathological abnormalities. Toward this end, tissue homogenates of post-mortem substantia nigra and amygdala tissues from PD, DLB and age-matched control donors were spotted onto nitrocellulose membranes and probed with either chBIIB054 (a murine IgG2a analog of BIIB054, used to minimize background staining of human IgG) or 9E4. Strikingly, chBIIB054 detected α-syn only in tissue homogenates from PD or DLB donors but not from age-matched controls. In contrast, 9E4 did not distinguish PD or DLB from controls. (Fig. 4A). Next, we performed immunohistochemical analysis on post-mortem tissue from temporal cortex and substantia nigra tissue of control and PD donors. chBIIB054

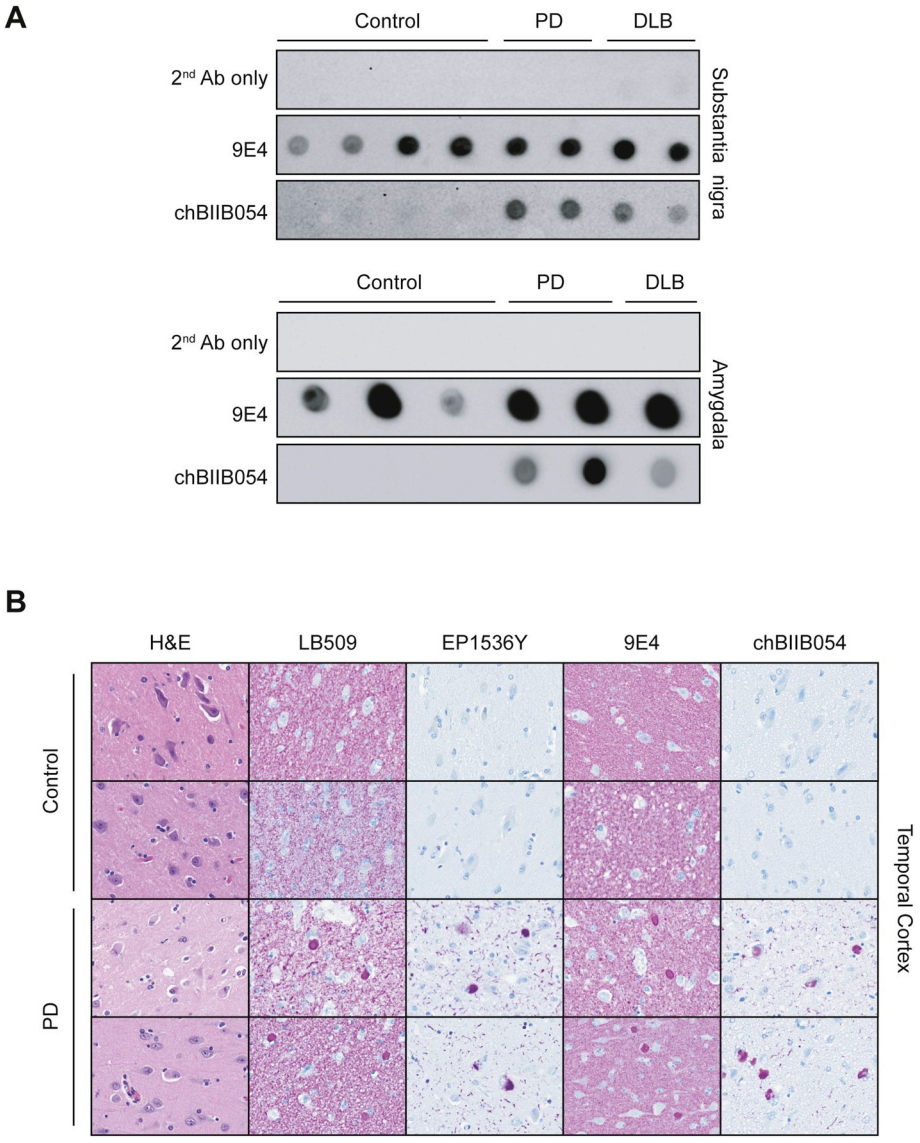

Fig. 4. BIIB054 selectively binds pathological α-syn in human tissue. (A) Dot blot analysis of post mortem substantia nigra (2 µg per dot, upper panel) and amygdala homogenates (0.2 µg per dot, lower panel) from control, PD and DLB tissues probed with chBIIB054, 9E4, and secondary antibody alone. (B) Immunohistochemistry staining of paraffin-embedded temporal cortex tissue from control and PD donors (purple) with chBIIB054, LB509 (total α-syn), EP1536Y (pSer129 α-syn) and 9E4 antibodies, and H&E staining.

showed robust staining for Lewy bodies, Lewy neurites and synaptic-like dots in tissue of PD and DLB patients, but did not stain tissues from control donors (Fig. 4B and Fig. S7). In contrast, LB509 and 9E4 detected Lewy pathology in PD tissue, but also showed prominent staining in control tissue, indicating that they bind efficiently to normal physiological α-syn (Fig. 4B and Fig. S7). The staining pattern with the pSer129 α-syn specific antibody EP1536Y was similar to that obtained with BIIB054, except for notable pSer129 α-syn staining in the substantia nigra of control donors (Fig. 4B and Fig. S7). Together the immunohistochemical and biochemical data show a consistent pattern of highly preferential binding of BIIB054 to pathological aggregated α-syn, such as that found in PD and DLB brain tissue, over the physiological α-syn found in non-diseased human brain.

3.6. Treatment with chBIIB054 improves PD-like phenotypes in α-syn PFF-inoculation mouse models

Intracerebral inoculation of α-syn PFFs into wild type and tg α-syn mice recapitulates key features of human PD including progressive propagation of α-syn pathology, motor impairments and loss of striatal DAT density (Koprich et al., 2017; Luk et al., 2012a; Luk et al., 2012b). To explore the therapeutic potential of BIIB054 in a disease setting, we tested if treatment with chBIIB054 could ameliorate such PD-like phenotypes in three different α-syn PFF-inoculation mouse models. For these studies, 30 mg/kg was administered because at this dose, chBIIB054 concentrations in the CNS are expected to remain above the EC_{90} for binding of BIIB054 to aggregated α-syn throughout the treatment (Brys et al., 2018; Wang et al., 2018). chBIIB054 was dosed intraperitoneally because of the high bioavailability of BIIB054 in mice with area under the curve (0–14 day) values following 10 mg/kg injections of 19,700 (i.v) and 19,900 (i.p.) µg × h/ml. In all studies, chBIIB054 treatment started prior to intrastriatal PFF inoculation. Detailed study outlines are provided in Table S3.

We first tested BIIB054 in heterozygous tg α-syn A53T (M83) mice inoculated with human α-syn PFFs for its impact on onset of motor symptoms and fatal paralysis. In this disease model, intrastriatal α-syn PFF inoculation results in amplification and spread of pathological α-syn to brainstem and spinal cord that is directly linked to onset of motor

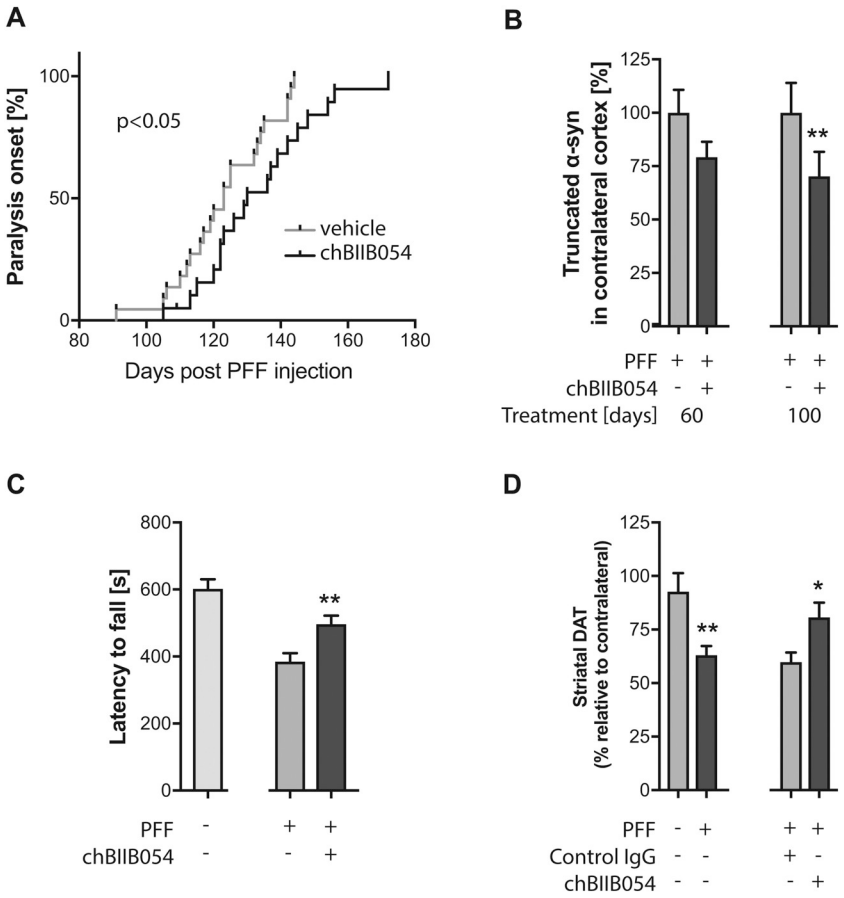

Fig. 5. chBIIB054 immunotherapy attenuates development of PD-like phenotypes in α-syn PFF-inoculation mouse models. (A) Kaplan-Meier plot for onset of paralysis symptoms in α-syn PFF-inoculated tg α-syn A53T (M83) mice treated with chBIIB054 (123 days) or vehicle (130 days; $p < 0.05$, log-rank test). (B) Levels of truncated α-syn-6 kDa fragment measured by western blotting in contralateral cortex of α-syn PFF-inoculated wild type mice that were treated with chBIIB054 or vehicle after 60 days ($p = 0.08$) or 100 days (** $p < 0.01$, mixed model). Western blot images for 100 day samples are shown in Fig. S10. (C) Wire hang performance of α-syn PFF-inoculated wild type mice treated with chBIIB054 or vehicle, measured as latency to fall from wire 60 days post PFF inoculation (** $p < 0.01$, Student's *t*-test). (D) *Left panel:* Quantitative DAT immunoblot analysis measuring ipsilateral relative to contralateral striatal DAT levels in α -syn A53T BAC transgenic mice 90 days post α-syn PFF injection. *Right panel:* Ipsilateral DAT density in α-syn PFF-inoculated α-syn A53T BAC transgenic mice treated with chBIIB054 or control IgG (* $p < 0.05$ and ** $p < 0.01$, Mann-Whitney test). Western blot images used for quantification are shown in Fig. S11. All values expressed as mean ± SEM.

symptoms and eventually fatal paralysis (Giasson et al., 2002; Luk et al., 2012b). When chBIIB054 was administered weekly in this model, a small but statistically significant delay was observed in median onset of first paralysis symptoms by 7 days (Fig. 5A), severe paralysis by 5 (Fig. S8A) and weight loss by 9 days (Fig. S8B). No symptoms were observed in heterozygous tg α-syn A53T (M83) mice without α-syn PFF inoculation at 8 months of age (not shown). These data show that chBIIB054 treatment can delay paralysis linked to α-syn spreading in this aggressive model. While the study wasn't designed to explore the impact of BIIB054 on biochemical readouts associated with PD pathology, western blot analysis of brainstem fractions of selected study animals that were euthanized due to severe paralysis showed strong pathology-associated signals for pSer129 α-syn and a truncated 6 kDa form of α-syn (Fig. S8C). pSer129 α-syn and the α-syn truncations were not detected in the control sample without PFF treatment.

We next tested if chBIIB054 treatment could reduce α-syn spreading and ameliorate motor impairment in α-syn PFF-inoculated wild type mice. Intrastriatal inoculation of murine α-syn PFFs led to increased levels of a truncated α-syn 6 kDa variant and pSer129 α-syn in the Triton X-100 insoluble fractions of the contralateral cortex, which were not observed in mice inoculated with monomeric murine α-syn (Fig. S9A). Truncated α-syn variants of similar size have been detected in PD/DLB but not in control brain tissue (Fig. S9B and C and (Li et al., 2005)). Although the molecular identity of the 6 kDa fragment is unknown, its reactivity with syn-1 antibody indicates that it contains residues 91–99 of α-syn (Perrin et al., 2003). pSer129 is a dominant pathological modification of α-syn (Anderson et al., 2006). pSer129 α-syn bands of varying molecular weights detected potentially correspond to ubiquitinated or oligomeric α-syn (Hasegawa et al., 2002; Volpicelli-Daley et al., 2014). Compared to vehicle-treated mice, treatment with chBIIB054 before and for up to 100 days after PFF inoculation resulted in a statistically significant 30% reduction of the ratio of 6 kDa α-syn variant/full length α-syn (Fig. 5B, Fig. S10, Table S3). Changes in pSer129 α-syn levels in the 100 day samples did not reach statistical significance after chBIIB054 treatment (Fig. S10A and B). Levels of pSer129 α-syn strongly correlated ($p < 0.01$) with levels of 6 kDa band (Fig. S10C). Treatment with chBIIB054 for 60 days trended to a ~20% reduction in the 6 kDa/full length α-syn ratio (Fig. 5B). Mice were further evaluated using the wire hang test to monitor subtle motor impairments (Luk et al., 2012a; Tran et al., 2014a). Mice treated with chBIIB054 for 60 days performed significantly better than vehicle-treated mice, reflected in a longer latency in time to fall from the wire (Fig. 5C). Compared to the performance of the vehicle-treated group, chBIIB054 treatment led to a ~ 50% improvement in this endpoint. These data demonstrate that BIIB054 treatment in α-syn PFF-inoculated wild type mice leads to reductions in levels of truncated α-syn 6 kDa variant and motor impairments.

Finally, we tested if chBIIB054 treatment could reduce the loss of DAT in tg α-syn A53T BAC mice inoculated with human α-syn PFFs. Loss of striatal dopamine nerve terminal function, a hallmark of PD, is reflected in decreases in DAT density that can be measured non-invasively in humans using DAT/SPECT imaging (Innis et al., 1993; Seibyl et al., 1995). Loss of DAT density has been recapitulated in α-syn PFF-inoculated wild type mice (Luk et al., 2012a). To test DAT density in a setting with human α-syn, we used PFF-inoculated tg α-syn A53T BAC mice that do not express murine α-syn (Kuo et al., 2010). Unilateral intrastriatal inoculation of human α-syn PFFs in these mice led to ~ 40% loss of ipsilateral striatal DAT levels (relative to contralateral site), as determined by densitometric analysis of Western blots (Fig. 5D). When tg α-syn A53T BAC mice were treated with chBIIB054 or control IgG (weekly, i.p., 30 mg/kg), before and after α-syn PFF inoculation for 3 months (see Table S3), the mice treated with chBIIB054 showed significantly smaller reductions of DAT density in ipsilateral striatum than observed in control IgG-treated mice (19% loss for

chBIIB054 vs 40% for control IgG, Fig. 5D and Fig. S11). Animals treated with control IgG displayed a similar extent of striatal DAT loss as observed in untreated α-syn PFF-inoculated mice (Fig. 5D). These data show that BIIB054 treatment can reduce loss of DAT density in a preclinical PD model.

4. Discussion

We describe here the identification and characterization of the α-syn antibody BIIB054, which is currently in a phase 2 clinical trial in individuals with PD. BIIB054 is a recombinant human IgG1 antibody generated from a library of memory B cells from elderly individuals without signs of neurological diseases. The same technology platform was previously used to generate aducanumab, an antibody targeting Aβ aggregates that is being developed for treatment of Alzheimer's Disease (Sevigny et al., 2016). BIIB054 was selected from a diverse panel of α-syn binding antibodies based on its specificity for α-syn, lack of binding to β- or γ-syn, and high selectivity for aggregated forms of α-syn that are believed to be responsible for PD disease progression.

Several antibodies against α-syn with apparent selectivity for oligomers, fibrils, or both over monomeric α-syn have been reported (Brannstrom et al., 2014; Covell et al., 2017; Lindstrom et al., 2014b; Nasstrom et al., 2011; Vaikath et al., 2015). Fast binding kinetics can make it difficult to quantify the relative affinities of these antibodies, which can appear to vary dramatically depending on the method of analysis. This is particularly true for measurements in those instances where binding is driven by avidity rather than affinity. The monovalent affinity of BIIB054 for recombinant α-syn was determined to be ~100 nM based on ITC using the monovalent BIIB054 Fab. Compared to the observed EC_{50} for recombinant fibrillar α-syn, measured by ELISA (120 pM), this suggests a relative selectivity for aggregates of at least 800-fold. Pronounced selectivity was also observed in the analysis of human tissue samples where BIIB054 only detected α-syn in PD and DLB, but not in control donors. Similar to what we reported previously for binding of aducanumab to Aβ (Arndt et al., 2018), BIIB054 likely discriminates between α-syn monomers and aggregates (including fibrils and oligomers) based on high avidity binding to aggregates, driven by its low affinity for monomeric α-syn and fast binding kinetics. This differs from other α-syn aggregate-selective antibodies, which were proposed to recognize specific conformational epitopes (Covell et al., 2017; Vaikath et al., 2015).

In contrast to BIIB054, we observed no difference in 9E4 binding to disease relative to control tissues, and only minimal selectivity for recombinant aggregates relative to α-syn monomer. PRX002, a humanized form of 9E4, recently was reported to be generally safe and tolerable in a phase 1 multiple ascending dose study and, like BIIB054, is in an ongoing phase 2 clinical study (Jankovic et al., 2018). Because of the differences in their selectivities for oligomeric and fibrillar α-syn aggregates relative to α-syn monomer, clinical data from BIIB054 and PRX002 will provide valuable insights into the optimal product profile for an α-syn therapeutic antibody.

Structure and epitope mapping studies provided detailed insights into the binding properties of BIIB054. First, we showed that BIIB054 bound to N-terminal residues 1–10 on α-syn. Unlike other α-syn antibodies targeting the N terminus, BIIB054 did not cross-react with β-syn, which is believed to be neuroprotective (Hashimoto et al., 2002; Uversky et al., 2002). The proximity of α-syn K10 in the structure with D50 on the BIIB054 light chain explains this selectivity, since K10 is replaced by a methionine in β-syn. Second, the crystal structure revealed direct contacts between BIIB054 and the acetyl group at the N terminus of α-syn, explaining the ~8-fold higher affinity of BIIB054 for N-terminal acetylated α-syn than unmodified α-syn. This is a relevant feature of the BIIB054 binding profile, since endogenous α-syn in human brain is predominantly acetylated at this site (Luth et al., 2015). Third, the structure revealed contacts of BIIB054 with M5 within a spacious pocket on BIIB054 that can accommodate oxidized methionine. This was confirmed by structural analysis of BIIB054 bound to α-$syn_{1–10}$ peptide oxidized at M5 (data not shown). Side-by-side binding studies of α-syn with and without M5 oxidation showed a slight increase in the affinity of BIIB054 for methionine oxidized α-syn. There is increasing evidence that oxidative stress is a contributing factor in PD. Indeed, α-syn deposits contain many oxidative post-translational modifications, including oxidation of all four methionines of α-syn (Chavarria and Souza, 2013; Schildknecht et al., 2013). Methionine oxidation promotes the formation of cytotoxic α-syn oligomers in vivo and in vitro (Carmo-Goncalves et al., 2014; Leong et al., 2009). Therefore, the ability of BIIB054 to bind oxidized forms of α-syn may be an additional attribute contributing to preferential recognition of pathological aggregated α-syn.

The selectivity of BII054 for aggregated α-syn suggests that the antibody was generated in response to misfolded α-syn. It is interesting to speculate that such antibodies may function as endogenous scavengers of pathological forms of α-syn and thus have a protective function. Consistent with this notion, the spacious pocket seen in the crystal structure surrounding M5 suggests that the endogenous precursor to BIIB054 may have been raised against Met-oxidized α-syn, which is deposited in Lewy pathology (Carmo-Goncalves et al., 2014; Schildknecht et al., 2013). Although we cannot exclude the possibility that BIIB054 is a naturally occurring autoantibody (nAb) that was generated from an antigen-independent response, the presence of 30 somatic hypermutations in BIIB054 relative to its closest germline sequences (data not shown) supports the idea that it was generated in response to α-syn. nAbs can be involved in maintenance of physiological homeostasis of their targets by e.g. clearing misfolded proteins (Lutz et al., 2009). Interestingly, serum levels of antibodies binding α-syn are reported to be lower in patients with PD (Besong-Agbo et al., 2013). In contrast, higher levels of antibodies targeting the C terminus of α-syn (residues 100–120) were found in cerebrospinal fluid (CSF) samples from PD patients than healthy controls (Akhtar et al., 2018). These antibodies targeting the C terminus of α-syn correlated with poor recognition but not necessarily with overall α-syn pathology burden. These findings raise the possibility that some α-syn antibodies may be protective, while others could be deleterious.

Evidence for beneficial therapeutic effects of chBIIB054 treatment was observed in three different α-syn PFF inoculation mouse models using both traditional and novel experimental endpoints. chBIIB54 treatment in the tg α-syn A53T BAC model (Kuo et al., 2010) preserved the dopamine terminals innervating the striatum, as indicated by the reduced loss of striatal DAT protein. In humans, loss of striatal dopamine nerve terminal function, a hallmark of PD, strongly correlates with decreased DAT levels. This finding, along with the results of the preclinical model reported here, supports the use of Ioflupane I^{123} (DaTscan™) imaging as a noninvasive readout of PD progression in clinical trials of potential α-syn targeting, disease-modifying PD therapies. Systemic administration of chBIIB054 in tg α-syn A53T (M83) mice inoculated with α-syn PFF delayed the onset of paralysis and weight loss, possibly by slowing propagation of α-syn pathology. To our knowledge this is the first report of a successful delay of paralysis with a pharmacological intervention in this model. The translatability of the relatively small effect size observed in this aggressive fast progressing model is unknown, but the data suggest that BIIB054 immunotherapy may have the potential to produce meaningful disease modifying effects in humans by slowing the course of disease.

There are several caveats of these in vivo studies that are worth noting. First, because chBIIB054 treatment started before PFF inoculation, we cannot formally distinguish whether chBIIB054 exerted its beneficial effects by blocking PFF uptake or preventing neuron-to-neuron transmission of endogenous α-syn pathology. The latter seems more plausible, since the α-syn PFFs used in these studies were injected locally at 5–10 mg/ml, making it unlikely that the local concentrations of chBIIB054 following systemic treatment (projected to be ≤1 μg/ml based on the dose (Wang et al., 2018)) would be sufficient to block

uptake of exogenous seeds. Second, although chBIIB054 treatment rescued motor impairments, the only endpoint directly related to neurodegeneration was the reduced loss of striatal DAT protein. Loss of TH-positive neurons was not assessed. Third, we were unable to establish a statistically significant treatment effect on pSer129 α-syn, in part due to a high degree of animal to animal variability in this endpoint. The α-syn 6 kDa variant we used as an endpoint, and which was significantly reduced relative to full-length α-syn upon treatment of PFF-inoculated mice with chBIIB054, was only found in human PD and DLB brains and in PFF inoculated mice and not in control tissues, and correlated significantly with levels of pSer129 α-syn. Additional studies will be required to identify the specific identity of this fragment, and to provide additional evidence establishing the validity of using it as a surrogate marker for α-syn pathology.

There are multiple mechanisms by which antibody treatment could impact the development of α-syn pathology in animal models and in human disease. Although intrastriatal inoculation of α-syn PFF induces α-syn pathology in anatomically connected areas, clear evidence for trans-synaptically transmitted pathology is lacking (Rey et al., 2016). Tran et al., (2014) demonstrated that anti-α-syn immunotherapy was efficacious in an intrastriatal α-syn PFF inoculation model even when antibody treatment started one week after PFF injection, at a time when α-syn pathology was already observed. Further, others have reported effects of anti-α-syn immunotherapy in tg models overexpressing α-syn, in which extracellular α-syn is not believed to contribute to the development of pathology in a major way (Games et al., 2014; Lindstrom et al., 2014a; Mandler et al., 2015; Masliah et al., 2005; Masliah et al., 2011). Thus, it is possible that antibodies could reduce α-syn pathology through alternative mechanisms not involving the spread of extracellular α-syn. It was postulated that α-syn antibodies could enter neurons to engage intracellular α-syn or form complexes with membrane-bound aggregated α-syn, which in turn gets internalized and degraded by an autophagy pathway (Masliah et al., 2005; Masliah et al., 2011). The exact mechanism of action of BIIIB054 and other α-syn immunotherapies might be model or antibody dependent, but engaging extracellular α-syn to prevent spreading is currently the most plausible mechanism for α-syn immunotherapy in humans. The evidence presented here showing beneficial effects in 3 independent spreading models provides encouraging evidence in support of targeting this pathway.

The blood brain barrier is a formidable obstacle for developing antibody drugs that target the CNS. Following systemic administration, only about 0.1% of antibody in blood gains access to the CNS (Shen et al., 2004), so for any therapeutic candidate it is important to consider the projected human exposure in context of the affinity and selectivity of the drug. The CSF/serum ratio of ~ 0.4% that was measured for BIIB054 in clinical samples from individuals with PD following IV administration is at the high end of reported ratios (Beigel et al., 2010; Brys et al., 2018; Siemers et al., 2010; Tran et al., 2014b). At the highest dose being used in the current BIIB054 phase 2 clinical trial (3500 mg), the predicted concentrations of BIIB054 in the CNS ($\leq 2\,\mu g/ml$) would result in preferential engagement of aggregated forms of α-syn without significant engagement of monomeric α-syn. α-syn aggregates in CSF are of very low abundance. Only recently has progress in protein amplification methods based on prion-like induced self-aggregation allowed detection of α-syn aggregates in CSF of PD and DLB patients (Fairfoul et al., 2016; Sano et al., 2018; Shahnawaz et al., 2017). These new methods might facilitate demonstration of target engagement of BIIB054 to aggregated α-syn in the CSF and/or interstitial fluid of PD patients.

The well-established genetic and pathological links between α-syn and PD support the use of targeted antibody-based therapies. The high selectivity for pathological forms of α-syn and N-terminal epitope of BIIB054 clearly differentiate this molecule from other clinical candidates targeting α-syn, and the preclinical data reported here support the continued development of BIIB054 for the treatment and prevention of PD. A multicenter, randomized, double blind, placebo-controlled Phase 2 clinical study to evaluate the dose-related safety, immunogenicity, pharmacokinetic profile, and pharmacodynamic effects of BIIB054 on the integrity of nigrostriatal dopaminergic nerve terminals is ongoing in individuals with early PD ("SPARK" NCT03318523). Clinical data from this and other studies will help guide the development of treatments for PD.

Competing interests

AW, YL, JWA, CQ, BAS, LS, GM, PA, WDH, JMC, RBP and PHW are current or former paid employees and/or shareholders of Biogen; AW, CH, JB, NC, LS, FM, RMN and JG are current or former paid employees and shareholders of Neurimmune AG.

Funding

This research received no specific grant from any funding agency in the public, commercial, or not-for-profit sectors.

Acknowledgements

We are grateful to Omar Quintero-Monzon, Tom Patterson, Shawn Weng, Ellen Garber, Cathy Hession, Brian Majors, Joe Amatucci, Konrad Miatkowski, Chris Bergeron, Dingyi Wen, Yuting Huang, Susan Foley, Sheng Feng, Ioana Combaluzier, Thomas Hofer, Marcel Maier, Maria Grazia Barenco, Sarah Mueller-Steiner, Dagmar Brunner, Gudrun Prehn, Esther Berli, Severine Megel, Petra Borter, Andreas Hagenbuch and Nadine Glassl for their contributions to this work and to Ken Rhodes, Tom Engber, Marion Wittmann, Chris Henderson and Werner Meier for their advice and input. Blood from healthy elderly individuals was provided by Christoph Hock (University of Zurich). Use of the Advanced Photon Source was supported by the U. S. Department of Energy, Office of Science, Office of Basic Energy Sciences, under Contract No. DE-AC02-06CH11357. Use of the LRL Collaborative Access Team (LRL-CAT) beam line facilities at Sector 31 of the Advanced Photon Source was provided by Eli Lilly & Company, which operates the facility.

Appendix A. Supplementary data

Supplementary data to this article can be found online at https://doi.org/10.1016/j.nbd.2018.10.016.

References

Adams, P.D., Afonine, P.V., Bunkoczi, G., Chen, V.B., Davis, I.W., Echols, N., Headd, J.J., Hung, L.W., Kapral, G.J., Grosse-Kunstleve, R.W., McCoy, A.J., Moriarty, N.W., Oeffner, R., Read, R.J., Richardson, D.C., Richardson, J.S., Terwilliger, T.C., Zwart, P.H., 2010. PHENIX: a comprehensive Python-based system for macromolecular structure solution. Acta Crystallogr. D Biol. Crystallogr 66, 213–221.

Akhtar, R.S., Licata, J.P., Luk, K.C., Shaw, L.M., Trojanowski, J.Q., Lee, V.M., 2018. Measurements of auto-antibodies to alpha-synuclein in the serum and cerebral spinal fluids of patients with Parkinson's disease. J. Neurochem. 145 (6), 489–503 (Jun, Epub 2018 Jun 10).

Anderson, J.P., Walker, D.E., Goldstein, J.M., de Laat, R., Banducci, K., Caccavello, R.J., Barbour, R., Huang, J., Kling, K., Lee, M., Diep, L., Keim, P.S., Shen, X., Chataway, T., Schlossmacher, M.G., Seubert, P., Schenk, D., Sinha, S., Gai, W.P., Chilcote, T.J., 2006. Phosphorylation of Ser-129 is the dominant pathological modification of alpha-synuclein in familial and sporadic Lewy body disease. J. Biol. Chem. 281, 29739–29752.

Arndt, J.W., Qian, F., Smith, B.A., Quan, C., Kilambi, K.P., Bush, M.W., Walz, T., Pepinsky, R.B., Bussiere, T., Hamann, S., Cameron, T.O., Weinreb, P.H., 2018. Structural and kinetic basis for the selectivity of aducanumab for aggregated forms of amyloid-beta. Sci. Rep. 8, 6412.

Beigel, J.H., Nordstrom, J.L., Pillemer, S.R., Roncal, C., Goldwater, D.R., Li, H., Holland, P.C., Johnson, S., Stein, K., Koenig, S., 2010. Safety and pharmacokinetics of single intravenous dose of MGAWN1, a novel monoclonal antibody to West Nile virus. Antimicrob. Agents Chemother. 54, 2431–2436.

Besong-Agbo, D., Wolf, E., Jessen, F., Oechsner, M., Hametner, E., Poewe, W., Reindl, M., Oertel, W.H., Noelker, C., Bacher, M., Dodel, R., 2013. Naturally occurring alpha-

synuclein autoantibody levels are lower in patients with Parkinson disease. Neurology 80, 169–175.
Braak, H., Del Tredici, K., Rub, U., de Vos, R.A., Jansen Steur, E.N., Braak, E., 2003. Staging of brain pathology related to sporadic Parkinson's disease. Neurobiol. Aging 24, 197–211.
Brannstrom, K., Lindhagen-Persson, M., Gharibyan, A.L., Iakovleva, I., Vestling, M., Sellin, M.E., Brannstrom, T., Morozova-Roche, L., Forsgren, L., Olofsson, A., 2014. A generic method for design of oligomer-specific antibodies. PLoS One 9, e90857.
Brettschneider, J., Del Tredici, K., Lee, V.M., Trojanowski, J.Q., 2015. Spreading of pathology in neurodegenerative diseases: a focus on human studies. Nat. Rev. Neurosci. 16, 109–120.
Brundin, P., Dave, K.D., Kordower, J.H., 2017. Therapeutic approaches to target alpha-synuclein pathology. Exp. Neurol. 298, 225–235.
Brys, M., Hung, S., Fanning, L., Penner, N., Yang, M., David, E., Fox, T., Makh, S., Graham, D., Cedarbaum, J.M., 2017. Randomized, double-blind, placebo-controlled, single ascending dose study of anti-alpha-synuclein antibody BIIB054 in healthy volunteers. In: 13th International Conference on Alzheimer's and Parkinson's Diseases, AD/PD 2017, Vienna, Austria.
Brys, M., Fanning, L., Penner, N., Yang, M., Welch, M., Koenig, E., David, E., Fox, T., Makh, S., Graham, D., Weihofen, A., Cedarbaum, J.M., 2018. Randomized, double-blind, placebo-controlled, single ascending dose study of anti-alpha-synuclein antibody BIIB054 in patients with Parkinson's disease. In: 70th Annual Meeting of the American Academy of Neurology, AAN 2018, Los Angeles, CA, United States.
Carmo-Goncalves, P., Pinheiro, A.S., Romao, L., Cortines, J., Follmer, C., 2014. UV-induced selective oxidation of Met5 to Met-sulfoxide leads to the formation of neurotoxic fibril-incompetent alpha-synuclein oligomers. Amyloid 21, 163–174.
Chartier-Harlin, M.C., Kachergus, J., Roumier, C., Mouroux, V., Douay, X., Lincoln, S., Levecque, C., Larvor, L., Andrieux, J., Hulihan, M., Waucquier, N., Defebvre, L., Amouyel, P., Farrer, M., Destee, A., 2004. Alpha-synuclein locus duplication as a cause of familial Parkinson's disease. Lancet 364, 1167–1169.
Chavarria, C., Souza, J.M., 2013. Oxidation and nitration of alpha-synuclein and their implications in neurodegenerative diseases. Arch. Biochem. Biophys. 533, 25–32.
Covell, D.J., Robinson, J.L., Akhtar, R.S., Grossman, M., Weintraub, D., Bucklin, H.M., Pitkin, R.M., Riddle, D., Yousef, A., Trojanowski, J.Q., Lee, V.M., 2017. Novel conformation-selective alpha-synuclein antibodies raised against different in vitro fibril forms show distinct patterns of Lewy pathology in Parkinson's disease. Neuropathol. Appl. Neurobiol. 43, 604–620.
Cronin, K.D., Ge, D., Manninger, P., Linnertz, C., Rossoshek, A., Orrison, B.M., Bernard, D.J., El-Agnaf, O.M., Schlossmacher, M.G., Nussbaum, R.L., Chiba-Falek, O., 2009. Expansion of the Parkinson disease-associated SNCA-Rep1 allele upregulates human alpha-synuclein in transgenic mouse brain. Hum. Mol. Genet. 18, 3274–3285.
Dehay, B., Bourdenx, M., Gorry, P., Przedborski, S., Vila, M., Hunot, S., Singleton, A., Olanow, C.W., Merchant, K.M., Bezard, E., Petsko, G.A., Meissner, W.G., 2015. Targeting alpha-synuclein for treatment of Parkinson's disease: mechanistic and therapeutic considerations. Lancet Neurol. 14, 855–866.
Dhillon, J.S., Riffe, C., Moore, B.D., Ran, Y., Chakrabarty, P., Golde, T.E., Giasson, B.I., 2017. A novel panel of alpha-synuclein antibodies reveal distinctive staining profiles in synucleinopathies. PLoS One 12, e0184731.
Duda, J.E., Giasson, B.I., Mabon, M.E., Lee, V.M., Trojanowski, J.Q., 2002. Novel antibodies to synuclein show abundant striatal pathology in Lewy body diseases. Ann. Neurol. 52, 205–210.
Emsley, P., Lohkamp, B., Scott, W.G., Cowtan, K., 2010. Features and development of Coot. Acta Crystallogr. Sect. D 66, 486–501.
Fairfoul, G., McGuire, L.I., Pal, S., Ironside, J.W., Neumann, J., Christie, S., Joachim, C., Esiri, M., Evetts, S.G., Rolinski, M., Baig, F., Ruffmann, C., Wade-Martins, R., Hu, M.T., Parkkinen, L., Green, A.J., 2016. Alpha-synuclein RT-QuIC in the CSF of patients with alpha-synucleinopathies. Ann. Clin. Transl. Neurol. 3, 812–818.
Games, D., Valera, E., Spencer, B., Rockenstein, E., Mante, M., Adame, A., Patrick, C., Ubhi, K., Nuber, S., Sacayon, P., Zago, W., Seubert, P., Barbour, R., Schenk, D., Masliah, E., 2014. Reducing C-terminal-truncated alpha-synuclein by immunotherapy attenuates neurodegeneration and propagation in Parkinson's disease-like models. J. Neurosci. 34, 9441–9454.
George, S., Brundin, P., 2015. Immunotherapy in Parkinson's disease: micromanaging alpha-synuclein aggregation. J. Parkinson's Dis 5 (3), 413–424.
Giasson, B.I., Duda, J.E., Quinn, S.M., Zhang, B., Trojanowski, J.Q., Lee, V.M., 2002. Neuronal alpha-synucleinopathy with severe movement disorder in mice expressing A53T human alpha-synuclein. Neuron 34, 521–533.
Goedert, M., 2015. NEURODEGENERATION. Alzheimer's and Parkinson's diseases: the prion concept in relation to assembled Abeta, tau, and alpha-synuclein. Science 349, 1255555.
Goedert, M., Spillantini, M.G., Del Tredici, K., Braak, H., 2013. 100 years of Lewy pathology. Nat. Rev. Neurol. 9, 13–24.
Hasegawa, M., Fujiwara, H., Nonaka, T., Wakabayashi, K., Takahashi, H., Lee, V.M., Trojanowski, J.Q., Mann, D., Iwatsubo, T., 2002. Phosphorylated alpha-synuclein is ubiquitinated in alpha-synucleinopathy lesions. J. Biol. Chem. 277, 49071–49076.
Hashimoto, M., Hsu, L.J., Rockenstein, E., Takenouchi, T., Mallory, M., Masliah, E., 2002. alpha-Synuclein protects against oxidative stress via inactivation of the c-Jun N-terminal kinase stress-signaling pathway in neuronal cells. J. Biol. Chem. 277, 11465–11472.
Horvath, I., Iashchishyn, I.A., Forsgren, L., Morozova-Roche, L.A., 2017. Immunochemical detection of alpha-synuclein autoantibodies in Parkinson's disease: correlation between plasma and cerebrospinal fluid levels. ACS Chem. Neurosci. 8, 1170–1176.
Ibanez, P., Bonnet, A.M., Debarges, B., Lohmann, E., Tison, F., Pollak, P., Agid, Y., Durr, A., Brice, A., 2004. Causal relation between alpha-synuclein gene duplication and familial Parkinson's disease. Lancet 364, 1169–1171.
Innis, R.B., Seibyl, J.P., Scanley, B.E., Laruelle, M., Abi-Dargham, A., Wallace, E., Baldwin, R.M., Zea-Ponce, Y., Zoghbi, S., Wang, S., et al., 1993. Single photon emission computed tomographic imaging demonstrates loss of striatal dopamine transporters in Parkinson disease. Proc. Natl. Acad. Sci. U. S. A. 90, 11965–11969.
Jankovic, J., Goodman, I., Safirstein, B., Marmon, T.K., Schenk, D.B., Koller, M., Zago, W., Ness, D.K., Griffith, S.G., Grundman, M., Soto, J., Ostrowitzki, S., Boess, F.G., Martin-Facklam, M., Quinn, J.F., Isaacson, S.H., Omidvar, O., Ellenbogen, A., Kinney, G.G., 2018. Safety and tolerability of multiple ascending doses of PRX002/RG7935, an anti-alpha-synuclein monoclonal antibody, in patients with Parkinson disease: a randomized clinical trial. JAMA Neurol 75 (10), 1206–1214 (Oct 1).
Jelcic, I., Combaluzier, B., Jelcic, I., Faigle, W., Senn, L., Reinhart, B.J., Stroh, L., Nitsch, R.M., Stehle, T., Sospedra, M., Grimm, J., Martin, R., 2015. Broadly neutralizing human monoclonal JC polyomavirus VP1-specific antibodies as candidate therapeutics for progressive multifocal leukoencephalopathy. Sci. Transl. Med. 7, 306ra150.
Kabsch, W., 2010. XDS. Acta Crystallogr. D Biol. Crystallogr 66, 125–132.
Koprich, J.B., Kalia, L.V., Brotchie, J.M., 2017. Animal models of alpha-synucleinopathy for Parkinson disease drug development. Nat. Rev. Neurosci. 18, 515–529.
Kruger, R., Kuhn, W., Muller, T., Woitalla, D., Graeber, M., Kosel, S., Przuntek, H., Epplen, J.T., Schols, L., Riess, O., 1998. Ala30Pro mutation in the gene encoding alpha-synuclein in Parkinson's disease. Nat. Genet. 18, 106–108.
Kuo, Y.M., Li, Z., Jiao, Y., Gaborit, N., Pani, A.K., Orrison, B.M., Bruneau, B.G., Giasson, B.I., Smeyne, R.J., Gershon, M.D., Nussbaum, R.L., 2010. Extensive enteric nervous system abnormalities in mice transgenic for artificial chromosomes containing Parkinson disease-associated alpha-synuclein gene mutations precede central nervous system changes. Hum. Mol. Genet. 19, 1633–1650.
Lee, S.J., Desplats, P., Sigurdson, C., Tsigelny, I., Masliah, E., 2010. Cell-to-cell transmission of non-prion protein aggregates. Nat. Rev. Neurol. 6, 702–706.
Leong, S.L., Pham, C.L., Galatis, D., Fodero-Tavoletti, M.T., Perez, K., Hill, A.F., Masters, C.L., Ali, F.E., Barnham, K.J., Cappai, R., 2009. Formation of dopamine-mediated alpha-synuclein-soluble oligomers requires methionine oxidation. Free Radic. Biol. Med. 46, 1328–1337.
Li, W., West, N., Colla, E., Pletnikova, O., Troncoso, J.C., Marsh, L., Dawson, T.M., Jakala, P., Hartmann, T., Price, D.L., Lee, M.K., 2005. Aggregation promoting C-terminal truncation of alpha-synuclein is a normal cellular process and is enhanced by the familial Parkinson's disease-linked mutations. Proc. Natl. Acad. Sci. U. S. A. 102, 2162–2167.
Lindstrom, V., Fagerqvist, T., Nordstrom, E., Eriksson, F., Lord, A., Tucker, S., Andersson, J., Johannesson, M., Schell, H., Kahle, P.J., Moller, C., Gellerfors, P., Bergstrom, J., Lannfelt, L., Ingelsson, M., 2014a. Immunotherapy targeting alpha-synuclein protofibrils reduced pathology in (Thy-1)-h[A30P] alpha-synuclein mice. Neurobiol. Dis. 69, 134–143.
Lindstrom, V., Ihse, E., Fagerqvist, T., Bergstrom, J., Nordstrom, E., Moller, C., Lannfelt, L., Ingelsson, M., 2014b. Immunotherapy targeting alpha-synuclein, with relevance for future treatment of Parkinson's disease and other Lewy body disorders. Immunotherapy 6, 141–153.
Luk, K.C., Kehm, V., Carroll, J., Zhang, B., O'Brien, P., Trojanowski, J.Q., Lee, V.M., 2012a. Pathological alpha-synuclein transmission initiates Parkinson-like neurodegeneration in nontransgenic mice. Science 338, 949–953.
Luk, K.C., Kehm, V.M., Zhang, B., O'Brien, P., Trojanowski, J.Q., Lee, V.M., 2012b. Intracerebral inoculation of pathological alpha-synuclein initiates a rapidly progressive neurodegenerative alpha-synucleinopathy in mice. J. Exp. Med. 209, 975–986.
Luth, E.S., Bartels, T., Dettmer, U., Kim, N.C., Selkoe, D.J., 2015. Purification of alpha-synuclein from human brain reveals an instability of endogenous multimers as the protein approaches purity. Biochemistry 54, 279–292.
Lutz, H.U., Binder, C.J., Kaveri, S., 2009. Naturally occurring auto-antibodies in homeostasis and disease. Trends Immunol. 30, 43–51.
Mandler, M., Valera, E., Rockenstein, E., Mante, M., Weninger, H., Patrick, C., Adame, A., Schmidhuber, S., Santic, R., Schneeberger, A., Schmidt, W., Mattner, F., Masliah, E., 2015. Active immunization against alpha-synuclein ameliorates the degenerative pathology and prevents demyelination in a model of multiple system atrophy. Mol. Neurodegener. 10, 10.
Masliah, E., Rockenstein, E., Adame, A., Alford, M., Crews, L., Hashimoto, M., Seubert, P., Lee, M., Goldstein, J., Chilcote, T., Games, D., Schenk, D., 2005. Effects of alpha-synuclein immunization in a mouse model of Parkinson's disease. Neuron 46, 857–868.
Masliah, E., Rockenstein, E., Mante, M., Crews, L., Spencer, B., Adame, A., Patrick, C., Trejo, M., Ubhi, K., Rohn, T.T., Mueller-Steiner, S., Seubert, P., Barbour, R., McConlogue, L., Buttini, M., Games, D., Schenk, D., 2011. Passive immunization reduces behavioral and neuropathological deficits in an alpha-synuclein transgenic model of Lewy body disease. PLoS One 6, e19338.
Nalls, M.A., Pankratz, N., Lill, C.M., Do, C.B., Hernandez, D.G., Saad, M., DeStefano, A.L., Kara, E., Bras, J., Sharma, M., Schulte, C., Keller, M.F., Arepalli, S., Letson, C., Edsall, C., Stefansson, H., Liu, X., Pliner, H., Lee, J.H., Cheng, R., International Parkinson's Disease Genomics Consortium, Parkinson's Study Group, Parkinson's Research: The Organized GENetics Initiative, 23andMe; GenePD, NeuroGenetics Research Consortium, Hussman Institute of Human Genomics, Ashkenazi Jewish Dataset Investigator, Cohorts for Health and Aging Research in Genetic Epidemiology, North American Brain Expression Consortium, United Kingdom Brain Expression Consortium, Greek Parkinson's Disease Consortium, Alzheimer Genetic Analysis Group, Ikram, M.A., Ioannidis, J.P., Hadjigeorgiou, G.M., Bis, J.C., Martinez, M., Perlmutter, J.S., Goate, A., Marder, K., Fiske, B., Sutherland, M., Xiromerisiou, G., Myers, R.H., Clark, L.N., Stefansson, K., Hardy, J.A., Heutink, P., Chen, H., Wood, N.W., Houlden, H., Payami, H., Brice, A., Scott, W.K., Gasser, T., Bertram, L., Eriksson, N., Foroud, T., Singleton, A.B., 2014. Large-scale meta-analysis of genome-

wide association data identifies six new risk loci for Parkinson's disease. Nat. Genet. 46, 989–993.
Nasstrom, T., Goncalves, S., Sahlin, C., Nordstrom, E., Screpanti Sundquist, V., Lannfelt, L., Bergstrom, J., Outeiro, T.F., Ingelsson, M., 2011. Antibodies against alpha-synuclein reduce oligomerization in living cells. PLoS One 6, e27230.
Perrin, R.J., Payton, J.E., Barnett, D.H., Wraight, C.L., Woods, W.S., Ye, L., George, J.M., 2003. Epitope mapping and specificity of the anti-alpha-synuclein monoclonal antibody Syn-1 in mouse brain and cultured cell lines. Neurosci. Lett. 349, 133–135.
Polymeropoulos, M.H., Lavedan, C., Leroy, E., Ide, S.E., Dehejia, A., Dutra, A., Pike, B., Root, H., Rubenstein, J., Boyer, R., Stenroos, E.S., Chandrasekharappa, S., Athanassiadou, A., Papapetropoulos, T., Johnson, W.G., Lazzarini, A.M., Duvoisin, R.C., Di Iorio, G., Golbe, L.I., Nussbaum, R.L., 1997. Mutation in the alpha-synuclein gene identified in families with Parkinson's disease. Science 276, 2045–2047.
Rey, N.L., George, S., Brundin, P., 2016. Review: spreading the word: precise animal models and validated methods are vital when evaluating prion-like behaviour of alpha-synuclein. Neuropathol. Appl. Neurobiol. 42, 51–76.
Sano, K., Atarashi, R., Satoh, K., Ishibashi, D., Nakagaki, T., Iwasaki, Y., Yoshida, M., Murayama, S., Mishima, K., Nishida, N., 2018. Prion-like seeding of misfolded alpha-synuclein in the brains of dementia with Lewy body patients in RT-QUIC. Mol. Neurobiol. 55 (5), 3916–3930 (May, Epub 2017 May 26).
Schenk, D.B., Koller, M., Ness, D.K., Griffith, S.G., Grundman, M., Zago, W., Soto, J., Atiee, G., Ostrowitzki, S., Kinney, G.G., 2017. First-in-human assessment of PRX002, an anti-alpha-synuclein monoclonal antibody, in healthy volunteers. Mov. Disord. 32, 211–218.
Schildknecht, S., Gerding, H.R., Karreman, C., Drescher, M., Lashuel, H.A., Outeiro, T.F., Di Monte, D.A., Leist, M., 2013. Oxidative and nitrative alpha-synuclein modifications and proteostatic stress: implications for disease mechanisms and interventions in synucleinopathies. J. Neurochem. 125, 491–511.
Schneeberger, A., Tierney, L., Mandler, M., 2016. Active immunization therapies for Parkinson's disease and multiple system atrophy. Mov. Disord. 31, 214–224.
Seibyl, J.P., Marek, K.L., Quinlan, D., Sheff, K., Zoghbi, S., Zea-Ponce, Y., Baldwin, R.M., Fussell, B., Smith, E.O., Charney, D.S., van Dyck, C., et al., 1995. Decreased single-photon emission computed tomographic [123I]beta-CIT striatal uptake correlates with symptom severity in Parkinson's disease. Ann. Neurol. 38, 589–598.
Sevigny, J., Chiao, P., Bussiere, T., Weinreb, P.H., Williams, L., Maier, M., Dunstan, R., Salloway, S., Chen, T., Ling, Y., O'Gorman, J., Qian, F., Arastu, M., Li, M., Chollate, S., Brennan, M.S., Quintero-Monzon, O., Scannevin, R.H., Arnold, H.M., Engber, T., Rhodes, K., Ferrero, J., Hang, Y., Mikulskis, A., Grimm, J., Hock, C., Nitsch, R.M., Sandrock, A., 2016. The antibody aducanumab reduces Abeta plaques in Alzheimer's disease. Nature 537, 50–56.
Shahnawaz, M., Tokuda, T., Waragai, M., Mendez, N., Ishii, R., Trenkwalder, C., Mollenhauer, B., Soto, C., 2017. Development of a biochemical diagnosis of Parkinson disease by detection of alpha-synuclein misfolded aggregates in cerebrospinal fluid. JAMA Neurol 74, 163–172.
Shen, D.D., Artru, A.A., Adkison, K.K., 2004. Principles and applicability of CSF sampling for the assessment of CNS drug delivery and pharmacodynamics. Adv. Drug Deliv. Rev. 56, 1825–1857.
Siemers, E.R., Friedrich, S., Dean, R.A., Gonzales, C.R., Farlow, M.R., Paul, S.M., Demattos, R.B., 2010. Safety and changes in plasma and cerebrospinal fluid amyloid beta after a single administration of an amyloid beta monoclonal antibody in subjects with Alzheimer disease. Clin. Neuropharmacol. 33, 67–73.
Singleton, A.B., Farrer, M., Johnson, J., Singleton, A., Hague, S., Kachergus, J., Hulihan, M., Peuralinna, T., Dutra, A., Nussbaum, R., Lincoln, S., Crawley, A., Hanson, M., Maraganore, D., Adler, C., Cookson, M.R., Muenter, M., Baptista, M., Miller, D., Blancato, J., Hardy, J., Gwinn-Hardy, K., 2003. alpha-Synuclein locus triplication causes Parkinson's disease. Science 302, 841.
Soldner, F., Stelzer, Y., Shivalila, C.S., Abraham, B.J., Latourelle, J.C., Barrasa, M.I., Goldmann, J., Myers, R.H., Young, R.A., Jaenisch, R., 2016. Parkinson-associated risk variant in distal enhancer of alpha-synuclein modulates target gene expression. Nature 533, 95–99.
Spillantini, M.G., Schmidt, M.L., Lee, V.M., Trojanowski, J.Q., Jakes, R., Goedert, M., 1997. Alpha-synuclein in Lewy bodies. Nature 388, 839–840.
Sugahara, M., Kunishima, N., 2006. Novel versatile cryoprotectants for heavy-atom derivatization of protein crystals. Acta Crystallogr. D Biol. Crystallogr D62, 520–526.
Tran, H.T., Chung, C.H., Iba, M., Zhang, B., Trojanowski, J.Q., Luk, K.C., Lee, V.M., 2014a. Alpha-synuclein immunotherapy blocks uptake and templated propagation of misfolded alpha-synuclein and neurodegeneration. Cell Rep. 7, 2054–2065.
Tran, J.Q., Rana, J., Barkhof, F., Melamed, I., Gevorkyan, H., Wattjes, M.P., de Jong, R., Brosofsky, K., Ray, S., Xu, L., Zhao, J., Parr, E., Cadavid, D., 2014b. Randomized phase I trials of the safety/tolerability of anti-LINGO-1 monoclonal antibody BIIB033. Neurol Neuroimmunol. Neuroinflamm 1, e18.
Uversky, V.N., Li, J., Souillac, P., Millett, I.S., Doniach, S., Jakes, R., Goedert, M., Fink, A.L., 2002. Biophysical properties of the synucleins and their propensities to fibrillate: inhibition of alpha-synuclein assembly by beta- and gamma-synucleins. J. Biol. Chem 277, 11970–11978.
Vagin, A., Teplyakov, A., 1997. MOLREP: an automated program for molecular replacement. J. Appl. Crystallogr. 30, 1022–1025.
Vaikath, N.N., Majbour, N.K., Paleologou, K.E., Ardah, M.T., van Dam, E., van de Berg, W.D., Forrest, S.L., Parkkinen, L., Gai, W.P., Hattori, N., Takanashi, M., Lee, S.J., Mann, D.M., Imai, Y., Halliday, G.M., Li, J.Y., El-Agnaf, O.M., 2015. Generation and characterization of novel conformation-specific monoclonal antibodies for alpha-synuclein pathology. Neurobiol. Dis. 79, 81–99.
Valera, E., Masliah, E., 2013. Immunotherapy for neurodegenerative diseases: focus on alpha-synucleinopathies. Pharmacol. Ther. 138, 311–322.
Volpicelli-Daley, L.A., Luk, K.C., Lee, V.M., 2014. Addition of exogenous alpha-synuclein preformed fibrils to primary neuronal cultures to seed recruitment of endogenous alpha-synuclein to Lewy body and Lewy neurite-like aggregates. Nat. Protoc. 9, 2135–2146.
Wang, Q., Delva, L., Weinreb, P.H., Pepinsky, R.B., Graham, D., Veizaj, E., Cheung, A.E., Chen, W., Nestorov, I., Rohde, E., Caputo, R., Kuesters, G.M., Bohnert, T., Gan, L.S., 2018. Monoclonal antibody exposure in rat and cynomolgus monkey cerebrospinal fluid following systemic administration. Fluids Barriers CNS. 15, 10.
Waxman, E.A., Duda, J.E., Giasson, B.I., 2008. Characterization of antibodies that selectively detect alpha-synuclein in pathological inclusions. Acta Neuropathol 116, 37–46.